HEAT AND MASS TRANSFER TO PALLING WATER DROPLET IN A STEAM ATMOSPHERE

by

Anozie C. Onyemaechi

B. Sc., University of Ife, Nigeria (1980)

Submitted in partial fulfillment of
the requirements for the Degree of

MASTER OF SCIENCE at the

MASSACHUSETTS INSTITUTE OF TECHNOLOGY

December 1983

© Massachusetts Institute of Technology 1983

Signature of Author: _____
Department of Nuclear Engineering

Certified by: _____
Thesis Supervisor

Accepted by: _____
Chairman, Nuclear Engineering Committee

HEAT AND MASS TRANSFER TO PALLING WATER IN A STEAM ATMOSPHERE

by

Anozie C. Onyemaechi

Submitted to the Department of Nuclear Engineering on December 16. 1983 in partial fulfillment of the requirements for the Degree of Master of Science.

ABSTRACT

The problem is the determination of the temperature and density distribution in a steam atmosphere surrounding a falling droplet. Prom the results thus obtained, the heat and mass fluxes are computed along with their respective transfer coefficients. Numerical computation is required and an explicit finite difference method is used in the reduction of the energy and mass equations into finite difference forms. The velocity distribution is obtained from the numerical solution of the viscous flow around a droplet at a Reynolds number of 1000. Prom this distribution, the eddy diffusivity distribution is obtained. The droplet model used is that of complete mixing, that is, the droplet is assumed to be vigorously mixed such that the temperature and density profile in the droplet is uniform. Computed results are compared with few available data and are found to be in good agreement.

Thesis Supervisor: M. W. Golay

Title: Associate Professor of Nuclear Engineering

TABLE OF CONTENTS

	Abstract	i
	Acknowledgement	ii
	Nomenclature	iii
1.	INTRODUCTION	1
2.	CALCULATION OF DROPLET TRAJECTORIES	11
3.	THEORETICAL FORMULATION	22
4.	NUMERICAL COMPUTATION	34
5.	DISCUSSION OF RESULTS	41
	CONCLUSION	68
	REFERENCES	69
	APPENDICES	72

ACKNOWLEDGEMENTS

The author extends his sincerest appreciation to his thesis supervisor, Professor M. W. Golay, for his invaluable assistance and support during the course of this study. His unique ability to motivate and direct, while at the same time, providing ample opportunity for development and exploration of ideas, has made the author's association with him an extremely rewarding experience.

I am deeply grateful to my wife, Pauline, for her patience, understanding, and moral support throughout the course of this study. Also, my heartfelt thanks go to my parents, to whom I am deeply indebted.

I gratefully acknowledge the Ahmady Bello University, Zaria, Nigeria for providing fellowship award that helped make this endeavor possible.

NOMENCLATURE

A_d	=	surface area of the droplet, (cm^2)
C	=	dimensional concentration of diffusing fluid
C_D	=	drag coefficient
C_p	=	heat capacity, (cal/g°K)
D	=	mass diffusivity, (cm^2/s)
d	=	droplet diameter, (cm)
g	=	gravitational constant, (cm/s^2)
h	=	heat transfer coefficient, ($cal/cm^2 s\ °K$)
h_{fg}	=	latent heat of vaporization, (cal/g)
K	=	thermal conductivity, (cal/cms°K)
K_g	=	mass transfer coefficients, (cm/s)
K1	=	Number of L1 printouts
L1	=	Number of time steps before printout
M	=	molecular weight
M_d	=	mass of the droplet, (g)
$\dot{m}''$	=	mass flux, ($g/cm^2 s$)
Nu	=	Nusselt number
P	=	total pressure, (atm)
P_a	=	partial pressure of air, (atm)
Pr	=	Prandtl number
P_v	=	partial pressure of water vapor,(atm)
$\dot{Q}''$	=	heat flux, ($cal/cm^2 s$)
r	=	radial distance from the surface of the droplet

R	=	droplet radius, (cm)
Re	=	Reynolds number
Sc	=	Schmidt number
Sh	=	Sherwood number
T	=	temperature, (°K)
t	=	time, (s)
U_r	=	radial velocity component, (cm/s)
$U_\infty(u_t)$	=	free-steam fluid velocity (terminal velocity), (cm/s)
U_θ	=	tangential velocity component, (cm/s)
V	=	kinematic viscosity, (cm^2/s)
α	=	thermal diffusivity, (cm^2/s)
ε_h	=	eddy diffusivity of heat, (cm^2/s)
ε_m	=	eddy diffusivity of momentum, (cm^2/s)
θ	=	spherical polar angle, measured from front stagnation
ρ	=	density, (g/cm^3)
σ	=	interfacial surface tension, (g/s^2)
τ	=	dimensionless time.

Subscripts

c	=	condensation
d	=	droplet
m	=	molecular
o	=	initial droplet condition

r	=	radial direction
s	=	droplet surface (interface) or sensible
t	=	turbulent
T	=	total
∞	=	far from droplet surface
θ	=	tangential direction

CHAPTER 1

INTRODUCTION

In recent times, there has been much interest in heat transfer, mass transfer, and motion of liquid drops in studies of combustion, condensation, absorption, and other technical processes where liquid drops exist. This latter category includes many processing operations employing liquid sprays such as the nuclear reactor emergency core cooling system. In line with this interest, substantial analytical study and experimentation have been done in determining the effectiveness of such liquid drops in the transfer processes. Significant portions of the droplets in sprays have Reynolds numbers on the order of 100; and models for such sprays are typically based on the behavior of individual droplets, which are assumed independent of each other. In general, we are concerned with the behavior of groups of droplets; however, the case of a single isolated droplet, which is considered in this study, is of fundamental importance in this regard and has long been a subject of investigation.

Cooling by use of water droplets takes place by simultaneous heat and mass transfer. A large heat transfer area per unit mass of water can be achieved by the formation of drops. The smaller the size of droplet the more the available specific heat transfer area, but the larger the possible drift loss. As such, drops with sizes on the order

of millimeters are widely used for industrial applications. Furthermore, the heat and mass exchanges during the passage of a droplet in a cooling system are of a transient nature. The complexity and interdependence of the phenomena precludes the possibility of a general analytical solution. However, approximate theoretical treatments of the problem that result in analytical solutions will be reviewed. The objective of the present study will be stated after the following literature review.

1.1 Literature Review

A number of works closely related to the subject of heat transfer to a single drop are incorporated in this review. An attempt will be made here to correlate available information on heat transfer to a fluid drop falling freely in a continuous medium and to draw upon pertinent information of mass transfer. The various theoretical approaches are discussed and the specific models and assumed mechanisms reviewed.

1.1.1 Continuous Phase

Under the category of the resistance in the continuous phase, the transport resistance is comparatively much larger than that in the dispersed phase and, therefore, the latter is neglected. Only the transport phenomena in the external flow field surrounding the sphere are usually analyzed. Konopliv and Sparrow (12) considered the unsteady thermal processes for a moving sphere which encounters a fluid

environment whose initial temperature is different from that of the sphere. However, the flow field is steady and Stokesian, Re<1, and the temperature field is transient and of the boundary layer type. In this continuous phase consideration, the thermal conductance of the solid sphere is usually high so that the surface temperature is spatially uniform and equal to the temperature in the sphere. Two conditions are usually considered: One is that of large heat capacity so that the sphere temperature is constant in time. In the other, the heat capacity of the sphere is not large so its temperature varies with time as a result of heat transfer with the fluid.

For a sphere accelerating in a fluid, the time for the hydrodynamic boundary layer to grow and reach steady state is on the order $tU_\infty/d=1$ (32). This means that the boundary layer growth is complete when the drop has moved a distance equal to its diameter. We are interested in the process over distances up to 500-1000 diameters; consequently, the widely used Ranz-Marshall (24) steady-state correlation may reasonably substitute for all the governing equations for the external field. The transient process (39) can be split into many steady state intervals if the quasi-steady state approach is appropriate. In this case, the governing equations for the external field of the drop was replaced by the steady-state analytical solutions which describes the heat and mass transfer to a sphere to obtain the transport resistance of the continuous phase.

1.1.2 Dispersed Phase

There exist several different models for the transport processes in the interior of the droplet. A common, and in some sense more general, procedure is based on deriving a correlation from an assumed theoretical model and verifying the assumption by means of experimental data. The following are three of such models in the literature:

1.1.2.1 Complete Mixing Model

In this model, the internal motion of the drop is so vigorous that complete mixing is achieved. The temperature profile in the drop is uniform and resistance to heat and mass transfer exists only in the continuous phase (39).

1.1.2.2 Non-mixing Model

This model assumes there is no internal motion and the equations of motion for the drop interior are removed and the energy equation is reduced to simply a transient heat conduction equation.

1.1.2.3 Mixing Model

Yao (39) proposed a new model which considered both the effects of oscillation and internal circulation on the mixing in the droplet. In order to solve the heat transport quantitatively, Yao assumed that the effects of heat transport due to the internal motion can be represented by the increase of the heat diffusivity, and this increase of heat diffusivity is linear and proportional to the sum of the maximum

Reynolds numbers of oscillations and internal circulations. The effective diffusivity was proposed to be

$$\alpha = \alpha_{\omega} \left[1+S \left(Re_{osc,max} + Re_{ic,max}\right)\right]$$

where S is a constant which shows the significance of internal mixing. $Re_{osc,max}$ and $Re_{ic,max}$ are the maximum Reynolds numbers for the oscillation and internal circulation respectively (15). α_{ω} is the diffusivity without any of these phenomena. He also used the Biot number

$$Bi = \frac{hR}{k_d}$$

to compare the external heat convection effect and the internal conduction of heat in the droplet. The result shows that the resistance due to the heat conduction in the droplet is important provided there is little or no mixing in the droplet. However, both the models for the external field and the interior field of the drop are important in describing the overall cooling phenomena.

Kronig and Brink (13) considered the case when the transport resistance is mainly in the spherical droplet and, in the droplet, the time of circulation is smaller than the diffusion time. Hadarmard (8) stream function was used to describe the internal circulation when the hydrodynamic conditions are unsteady. The transient cases of extreme Reynolds number, either very large or very small were solved by Ruckenstein (30) and Chao (3). In all these cases, the hydrodynamic conditions are in steady state. The droplet initially at uniform

temperature meets a constant temperature environment; internal circulation was considered, and at the interface the droplet velocity was given equal to the adjacent potential flow velocity.

1.1.3 Experimentation

Several investigators have measured the heat and mass exchanges in a variety of experimental situations. In most of these experiments a droplet or a small solid sphere is suspended by thin wires in a fluid flow. The variation of the droplet temperature in time is then measured, or alternatively the droplet is maintained at steady state by feeding it with the required heat or mass. Some of these experiments are reviewed below.

Frossling (5) reported the evaporation of drops of liquid for Reynolds numbers of 2 to 1000 and got the result

$$Sh = 2 + 0.552\ Re^{1/2}\ Sc^{1/3},$$

for droplets at steady hydrodynamic conditions with the temperature profiles in the drops assumed uniform and constant at all times. Ranz and Marshall (24) obtained the widely used formulae

$$Nu = 2 + 0.6\ Re^{1/2}\ Pr^{1/3}$$

$$Sh = 2 + 0.6\ Re^{1/2}\ Sc^{1/3}$$

for Reynolds number of 0 to 200, with the largest drop being 1.8mm in diameter. Lee and Ryley (18) considered the case of the evaporation of water drops in superheated steam and obtained

$$Nu = 2 + 0.74\ Re^{1/2}\ Pr^{1/3}$$

Powell (23) also reported an experimental data on the evaporation of water from spherical surface for Reynolds numbers of 650 to 4500. Rowe (29) reviewed the experimental work performed with solid spheres before 1965. By a statistical study of the experimental data they concluded that the correlation

$$Nu = 2 + A_2\ Re^{1/2}\ Pr^{1/3}$$

gives the best fit. The value of A_2 is given as 0.69 for air and 0.79 for water. The value of the exponent of the Reynolds number varies between 0.4 at Re = 1 and 0.6 at Re = 10^4, but an average value of 1/2 seems adequate in the range $20<Re<2000$.

Yao (39) designed an experiment to provide data on the relationship between the mean temperature of the drop and its position in free fall for different drop size, initial drop temperature and the temperature and humidity of the air through which it falls. His experiment, briefly, consists of a drop generator, a plastic column 3m in height containing conditioned air, and conditioning equipment, and a calorimeter that could be positioned at any elevation to catch and measure mean drop temperature. For photographic measurements a small amount of oil-free white water colour paint was added to the water. This has been shown to have negligible effect on surface tension but produced good light scattering within the drops.

E. Kulic et al. (14) experimental results obtained in

single droplet temperature response are applied to the problem of predicting the pressure drop in a dousing chamber containing an air/steam mixture. Their paper deals with an approach to predict the heat transfer effects associated with water droplets falling through the mixture of air/steam. They observed that the speed of response of the droplet temperature is much faster for droplets in saturated mixtures of 0.5 volume fraction of steam than for a 0.05 volume fraction of steam in the mixture and concluded that the temperature and mass transfer driving forces are greater at higher concentrations of steam in the mixture.

Another interesting experimental investigation is that of Brown (2), who investigated the rates of heat transfer to water sprays. The procedure for the heat transfer measurements involved the spraying of water from a number of nozzles in the head of a vertical cylinder to which steam was supplied. The inlet and exit water temperature were measured and, from these, knowing the feed rate, the total heat input was obtained and used to calculate the rate at which heat was transferred to the surface of the drops. The experiments also showed that the final temperature rise of the droplet is a linear function of drop diameter. Brown also pointed out that the reduction in temperature rise brought about by the presence of air was caused by a layer of air clinging to the drops creating a resistance, and the surface heat transfer process became one of diffusion rather than that of pure condensation. His experimental results are summarized in Fig. 1.1.

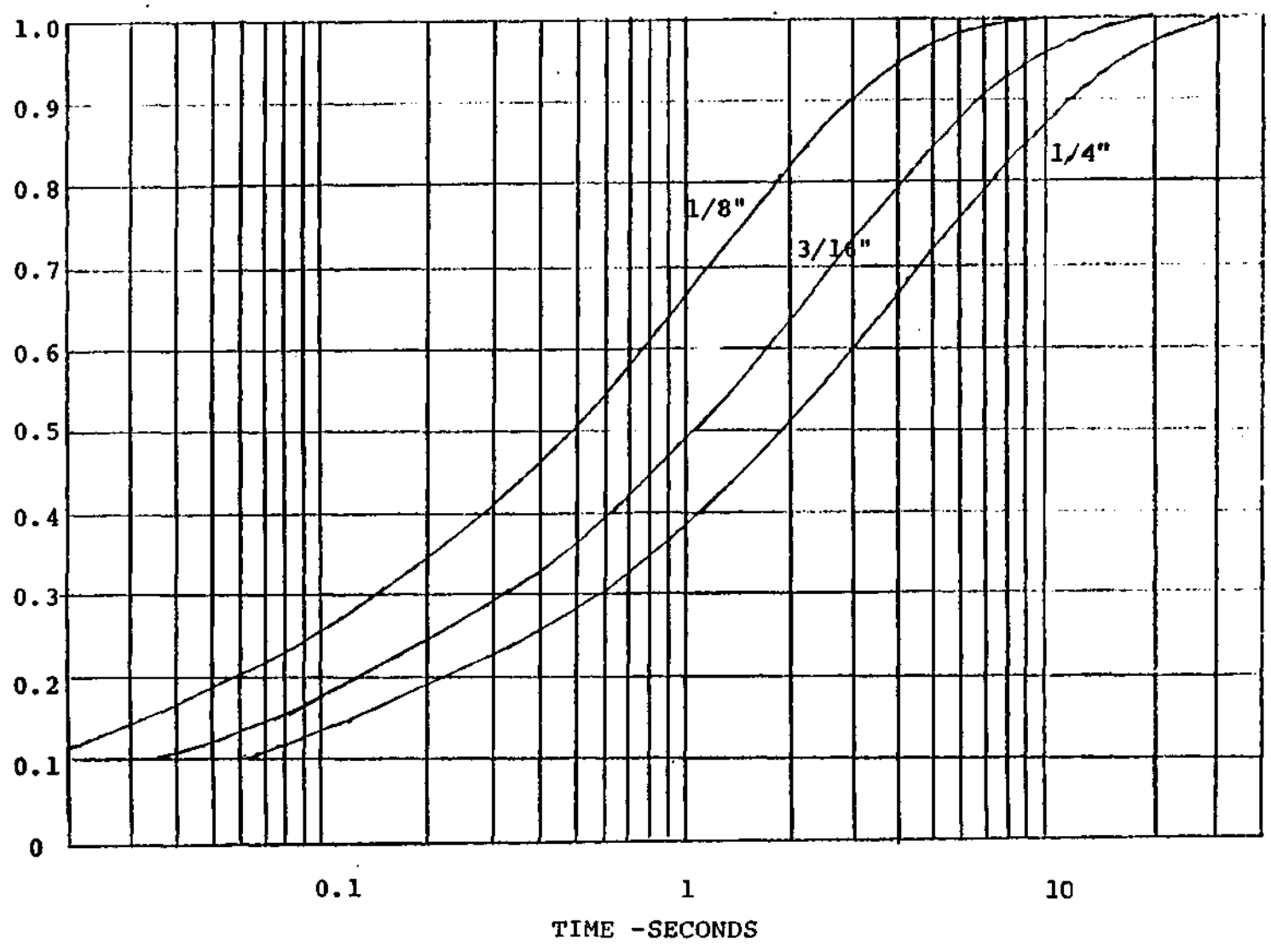


FIGURE 1.1 TIME OF HEATING OF A SPHERE OF WATER DROPLET(2)

1.2 Objective of the Present Study

Having completed the review of the theoretical and experimental studies to date, it was observed that little has been done in attacking the problem in question by computational methods. A numerical investigation of unsteady heat transfer to water droplet is thus worthwhile and is, therefore, presented in this study. However, among the various models mentioned, the complete mixing model is most appropriate for our problem since the resistance to heat transfer exists only in the continuous phase. In line with this objective, the temperature distribution around the droplet as a function of time will be computed along with the heat and mass transfer coefficients. A flexible computer program is developed which can be used for any droplet transfer process problem as long as the Reynolds number range criterion ($Re>1000$) is adhered to. The results obtained in this study are at Reynolds number of about 1000.

CHAPTER 2

CALCULATION OF DROPLET TRAJECTORIES

Since counterflow operation with an upward flow of fluid and a downward directed jet of droplets of a spray is most often encountered in practice, such a system will be considered for the motion of a single droplet in a continuous phase of infinite extent. Considering a solid sphere model projected vertically through a fluid, it either accelerates or decelerates until the gravitational force is counterbalanced by the frictional drag of the fluid. The equation for the net force acting on the sphere is:

$$F = \frac{\pi d^3}{6}(\rho_o - \rho_\infty)g - C_D \frac{\pi d^2}{4} \rho_\infty \frac{u^2}{2} \qquad (2.1)$$

where $\rho_\infty u^2 / 2$: kinematic pressure of the fluid;

$\frac{\pi d^3 \rho_o}{6}$: mass of the sphere;

g: local acceleration of gravity.

Then the acceleration of the sphere is

$$\frac{du}{dt} = \frac{g(\rho_o - \rho_\infty)}{\rho_o} - \frac{3C_D \rho_\infty u^2}{4d\rho_o} \qquad (2.2)$$

If, as is usual, $\rho_o >> \rho_\infty$, then

$$dt = \frac{du}{g - \frac{3C_D \rho_\infty u^2}{4d\rho_o}} \qquad (2.3)$$

2.1 Terminal Velocity and Drag Coefficient

When F in Eq. 2.1 is zero, the sphere has reached its terminal velocity and Eq. 2.3 may be rearranged and divided by μ^2 to give

$$\Phi = \frac{4d^3\rho_o\rho_\infty g}{3\mu^2} = C_D \left(\frac{du\rho_\infty}{\mu}\right)^2 \qquad (2.4)$$

The solid curve of Fig. 2.1 is a plot of Re vs Φ for rigid spheres, as computed by Lapple and Shepherd (17) on the basis of the solid line in Fig. 2.2. The terminal velocity of any rigid sphere having motion relative to the fluid can be determined as a function of its diameter, the density, and the acceleration by solving Eq. 2.4 for Φ and determining the terminal Reynolds number, Re_t, from Fig. 2.1 and calculating the terminal velocity, u_t, from the definition

$$u_t = \frac{\mu Re_t}{d\,\rho_\infty} \qquad (2.5)$$

The time of acceleration or deceleration of a rigid sphere from any velocity u to a velocity as near to u_t as desired can be determined by integration of Eq.2.3. Inspection of the integral form of Eq. 2.3, however, shows that an infinite time is required to attain exactly u_t, since at the terminal velocity

$$g - \frac{3C_D\rho_\infty u_t^2}{4d\rho_o} = 0 \qquad (2.6)$$

However, the data of a number of early investigators (1,7,19) on rain and artificially-produced water drops show that water drops larger

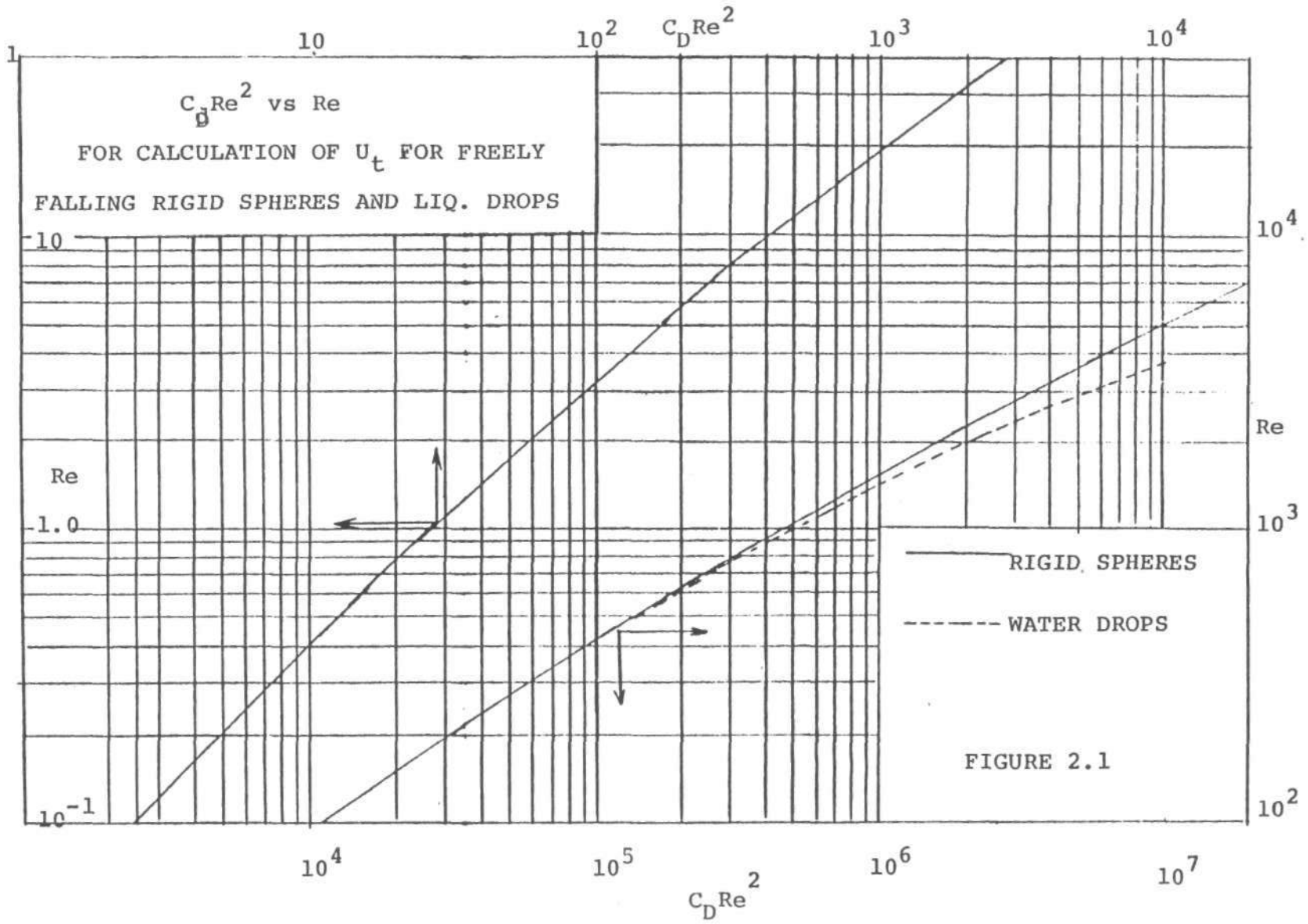

$C_g Re^2$ vs Re
FOR CALCULATION OF U_t FOR FREELY
FALLING RIGID SPHERES AND LIQ. DROPS
1
10
10^2
$C_D Re^2$
10^3
10^4
Re
1.0
10^{-1}
10^4
10^5
10^6
10^7
$C_D Re^2$
RIGID SPHERES
WATER DROPS

FIGURE 2.1

than 2mm. in diameter fall freely through air at terminal velocities less than those predicted by using drag coefficients for equivalent rigid spheres. The most complete data on the fall velocity of water drops and rain drops are those from the experiments of Law (16), who measured velocities of fall from rest for drops 1.25 to 6.1 mm. in diameter at intervals from 0.45 to 20 m below the point of rest. Smooth curves of his data are shown in Figs. 2.2 and 2.3, and values of C_D calculated from these data are shown as the dashed line in Fig. 2.1. The fundamentals of droplet motion are generally, in the absence of the above procedure, expressed in terms of a plot of drag coefficient versus Reynolds number. Such curves have been determined for solid spheres by numerous experimenters (28,36,37,40). Fig. 2.2 presents average curves for various shaped particles while the values upon which the curve for spherical particle was based are given in Table 2.1. However, there is somewhat less accurate formula of Dickinson and Marshall (4)

$$C_D = 0.22 + \frac{24}{Re}\left(1 + 0.15\, Re^{0.6}\right) \tag{2.7}$$

which gives results in the range $0<Re<3000$. The information so far presented applies to a single droplet in an infinite medium. The corrections that are necessary to account for the presence of neighboring droplets can, however, be estimated (6,9).

2.2 Previous Efforts to Predict Distortion

In addition to the fact that falling drops do not follow the free fall law over the entire distance of fall, they also do not remain

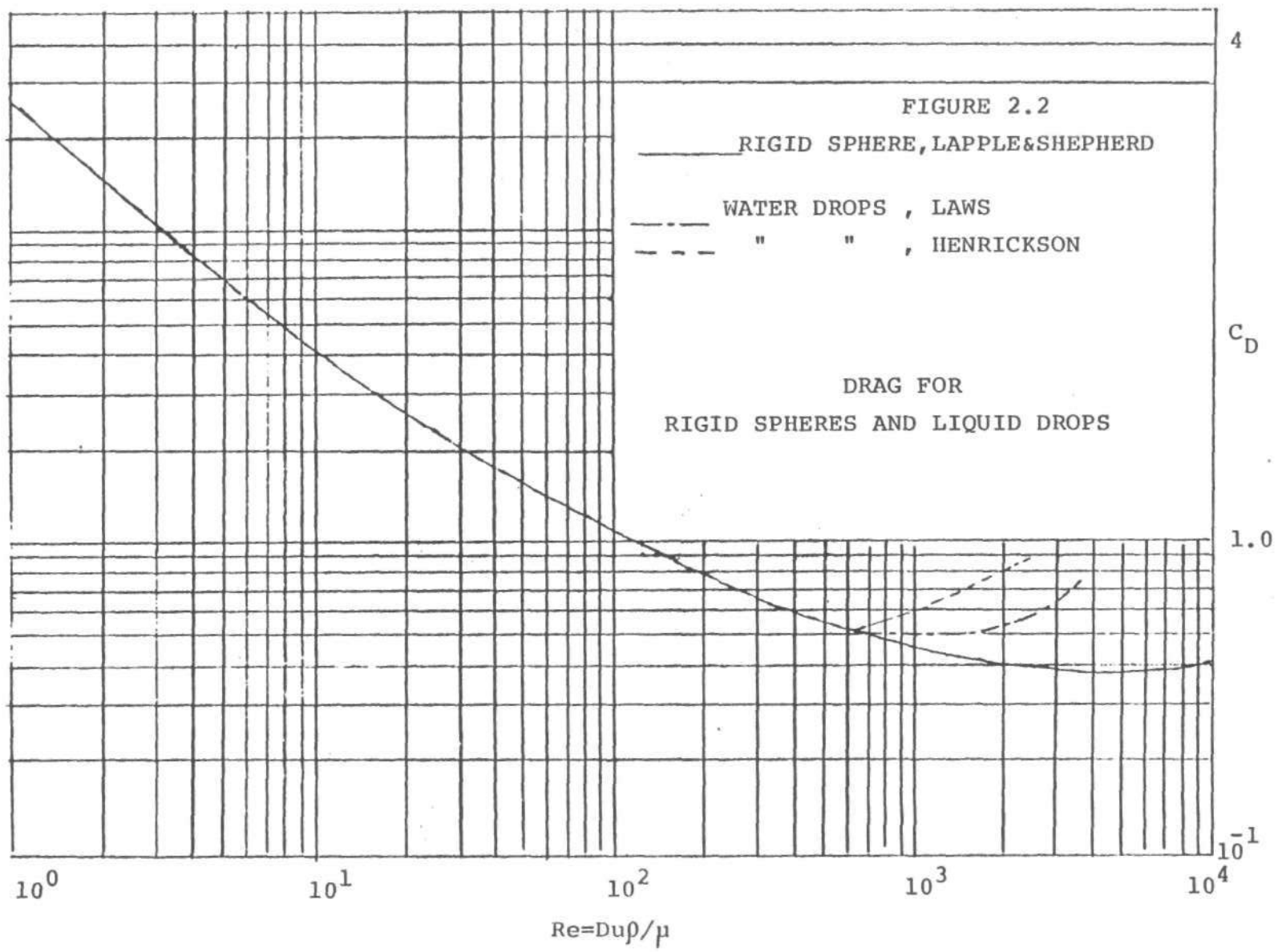


FIGURE 2.2

_____RIGID SPHERE, LAPPLE&SHEPHERD

_·_·_ WATER DROPS , LAWS

_ _ _ " " , HENRICKSON

DRAG FOR
RIGID SPHERES AND LIQUID DROPS

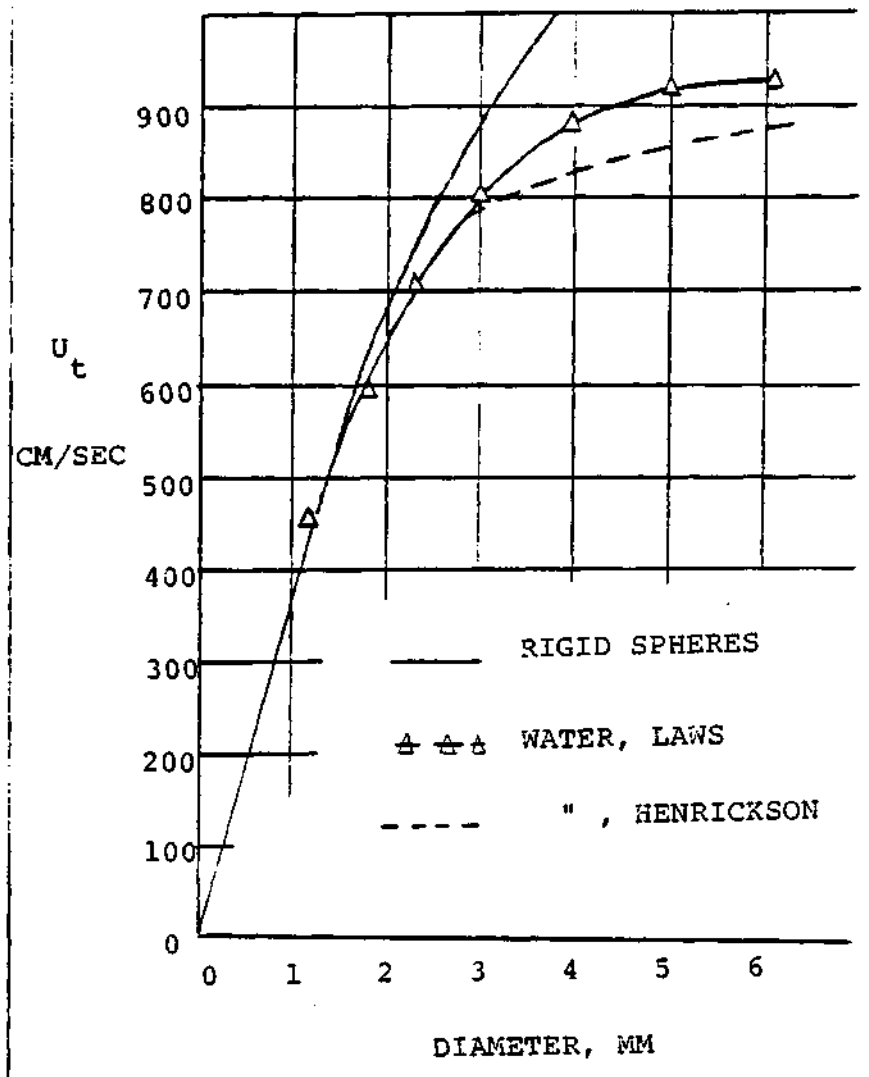
Table 2.1

VALUES OF DRAG COEFFICIENT FOR SPHERICAL PARTICLES

Re	C_D	C_DRe	C_DRe^2
0.1	240	24.0	2.4
0.2	120	24.0	4.8
0.3	80	24.0	7.2
0.5	49.5	24.8	12.4
0.7	36.5	25.6	17.9
1.0	26.5	26.5	26.5
2	14.4	28.8	57.6
3	10.4	31.2	93.7
5	6.9	34.5	173
7	5.4	37.8	265
10	4.1	41.0	410
20	2.55	51.0	1.02×10^3
30	2.00	60.0	1.80
50	1.50	75.0	3.75
70	1.27	89.0	6.23
100	1.07	107	10.7
200	0.77	154	30.8
300	0.65	195	58.5
700	0.50	350	245
1000	0.46	460	460
2000	0.42	840	1.68×10^6
3000	0.40	1200	3.60
5000	0.385	1920	9.60
7000	0.390	2730	19.1
10000	0.405	4050	40.5
20000	0.45	9000	180
30000	0.47	14200	426
50000	0.49	24500	1.23×10^9
70000	0.50	35000	2.45
100000	0.48	48000	4.8
200000	0.42	84000	16.8
300000	0.20	60000	18.0
400000	0.084	33600	13.4
600000	0.10	60000	36.0
1000000	0.13	130000	130
3000000	0.20	600000	1.8×10^{12}

FIGURE 2.3

TERMINAL VELOCITIES



perfect spheres. Saito (31) demonstrated mathematically that, for the case of water droplets falling through air, the forces acting on the drops tend to deform them into spheroids, oblate normal to the direction of motion. Lenard (19) showed that raindrops which are initially spherical take the shape of inverted cups at velocities from 6 to 8 meters per second and finally burst into fragments. The disrupting velocity varies from 20 to 10 meters per second for drops from 2.5 to 6mm. in diameter, respectively. Others (1,22) have shown that droplets falling feely reach a terminal velocity much less than that predicted from Stokes' law when the drop is more than 2mm. in diameter. In the more useful and interesting range of intermediate and high Reynolds numbers, Spilhaus' approach (35) has considerable promise. He suggested that the force tending to separate the drop laterally can be considered as proportional to both the area over which it acts and to the kinetic energy head, $\rho_\infty u^2/2$ of the continuous phase. The dimensionless proportionality factor, termed the distortion coefficient, similar to the drag coefficient, was assumed constant by Spilhaus.

Using the observed terminal velocities for a given size of drop, it is possible to calculate the maximum deformation that may occur when there is a flattening normal to the direction of motion. Levich (20) studied the influence of internal circulation and flattening of droplets. By means of these approximations and the terminal velocities mentioned above, the ratio of the deformed diameter to the original diameter can be etimated (11). Using the method of graphical

integration, the velocity and the distance traveled were calculated for different drop size, assuming no drop deformation. The results (11) showed that there would be only a 3 percent increase in the time of fall of spherical drops over that calculated for unresisted fall. In the same manner, the velocity and time of fall of drops, allowing for the deformation, can be calculated using Eq.2.3 if data are available on the magnitude of the deformation. When a droplet has reached its terminal velocity, with deformation occurring, the forces acting upon it are in equilibrium, then using Eq. 2.2, we have the equialent diameter given as

$$de = \left(\frac{4\rho_o g d^3}{3C_D \rho_\infty u_t^2}\right)^{1/2} \qquad (2.8)$$

Solution for de was accomplished by trial and error method, and it was noticed that the drag coefficient changes slowly with Reynolds number in the range where the diameter change is largest. Table 2.2 shows the results of such a calculation of the maximum deformation based on observed terminal velocities. The ratio of the deformed diameter to the original diameter plotted against the size of the drop is shown in Fig. 2.4. Thus, within the range of velocities of interest, the deformation (de-d) is proportional to the square of the velocity, the proportionality constant can be evaluated for any droplet size from the curve in Fig. 2.4.

Table 2.2

DEFORMATION OF FREELY FALING DROPS

Drop Diameter D	Velocity, cm/sec		Re from Observed U and D	C_D
	Observed	Calculated for Deformation		
0.1	32	32	2	14.00
0.2	130	125	16	3.20
0.4	180	180	45	1.50
1.0	395	395	246	0.73
2.0	577	620	723	0.52
2.5	640	715	1000	0.49
3.0	692	822	1300	0.44
4.5	800	946	2250	0.40
5.5	800	1080	2720	0.39
6.0	800	1300	3000	0.38

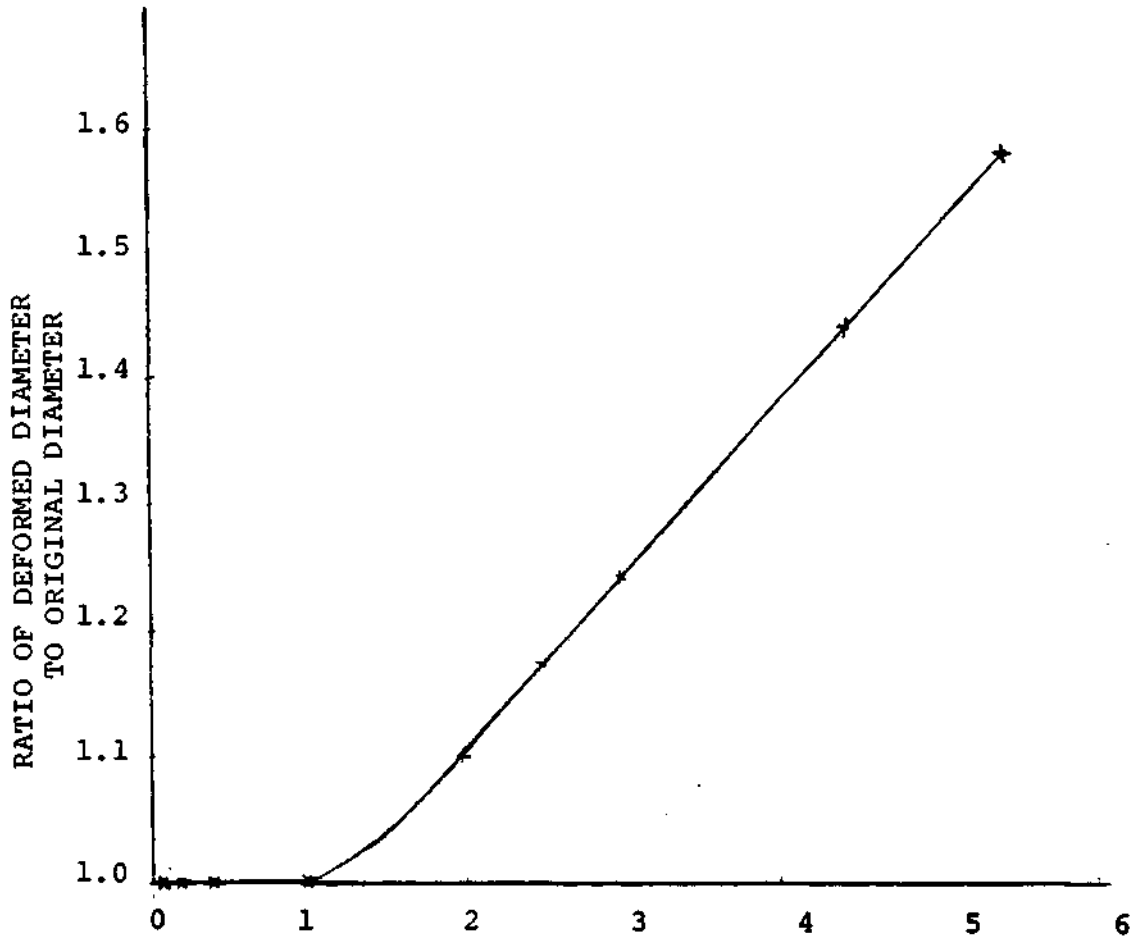


FIGURE 2.4 DROP DEFORMATION AS CALCULATED FROM TERMINAL VELOCITIES

CHAPTER 3

THEORETICAL FORMULATION

3.1 Problem Statement

Consider a droplet of radius R, initially at a uniform temperature T_o, and falling at a constant velocity u_t (terminal velocity) in an air-steam medium of infinite extent, which has a temperature T_∞, higher than that of the droplet. The problem is to use the method of numerical computation in predicting the rate of heat pick-up by the falling droplet in a mixture of air and steam. The falling droplet experiences two unidirectional heat fluxes directed towards its surface; one caused by the temperature difference acting as a driving force between the surroundings and itself; the second caused by the steam concentration difference in the bulk and at the droplet surface acting as a mass transfer driving force. These components comprise the total heat which is exchanged between the surroundings and the droplet. This problem is to be solved in terms of the temperature or concentration distribution around the droplet. The flow field vis-a-vis the velocity components have been computed and remain unaltered as long as the conditions under which it was obtained remain unchanged.

3.1 Assumptions

In order to solve the problem fairly readily, we have to make several simplifying assumptions. These are as follows:

3.2.1 Completely mixed model. This means that the internal

resistance to heat transfer of the droplet is negligible compared to the external gas phase resistance. This assumption implies that there is no temperature gradient within the droplet. Thus the rate of heat transfer to the droplet is equal to the rate of heat absorption by the droplet.

3.2.2 The droplet is assumed to be falling at its terminal velocity.

3.2.3 The far-field temperature of the continuous phase is presumed to remain constant during the drop's lifetime.

3.2.4 The density and the thermal conductivity of the droplet are constant.

3.2.5 Viscous dissipation is negligible and symmetry of revolution obtains for all dependent variable fields.

3.2.6 The effect of condensation upon the droplet diameter is ignored.

3.2.7 Absence of droplet oscillation. The occurrence of droplet oscillation was studied and reported (38). It has been shown that if the Weber number ($U_t^2 d\rho_\infty/\sigma$) is less than 4, the droplet would exhibit little oscillation and the assumption of absence of oscillation will be justified. This criterion is satisfied in this study.

3.3 Governing Equations

The governing equtions which describe the energy, and mass transport at the exterior of the falling drop are formulated below considering the assumptions made. The equtions for $r \geq R$ are the following:

Continuity:

$$\frac{1}{r^2}\frac{\partial}{\partial r}(r^2 u_r) + \frac{1}{r\sin\theta}\frac{\partial}{\partial \theta}(u_\theta \sin\theta) = 0 \qquad (3.1)$$

Energy:

$$\rho C_p\left(\frac{\partial T}{\partial t} + U_r\frac{\partial T}{\partial r} + \frac{U_\theta}{r}\frac{\partial T}{\partial \theta}\right) = k\left[\frac{1}{r^2}\frac{\partial}{\partial r}\left(r^2\frac{\partial T}{\partial r}\right) + \frac{1}{r^2\sin\theta}\frac{\partial}{\partial \theta}\left(\sin\theta\frac{\partial T}{\partial \theta}\right)\right] \qquad (3.2)$$

Mass(vapor concentration)

$$\frac{\partial C}{\partial t} + U_r\frac{\partial C}{\partial r} + \frac{U_\theta}{r}\frac{\partial C}{\partial \theta} = D\left[\frac{1}{r^2}\frac{\partial}{\partial r}\left(r^2\frac{\partial C}{\partial r}\right) + \frac{1}{r^2\sin\theta}\frac{\partial C}{\partial \theta}\left(\sin\theta\frac{\partial C}{\partial \theta}\right)\right]. \qquad (3.3)$$

The velocity components, U_r, and U_θ are found from the numerical flow solution of Rimon and Cheng (26) and the stream lines at Reynolds number of 1000 from which these components are computed as shown in Fig. 3.1. The computed velocity components are shown in Tables 5.6 - 5.7. In the case considered resistance to transfer is present in the external fluid only and this velocity distribution remains valid as long as Reynolds number condition is satisfied. A mass balance on an elemental cell in the streamline, considering bulk flow in both the radial and tangential directions, gives rise to the computed velocity components. (See Appendix D for calculation technique).

$R_e = 1000$

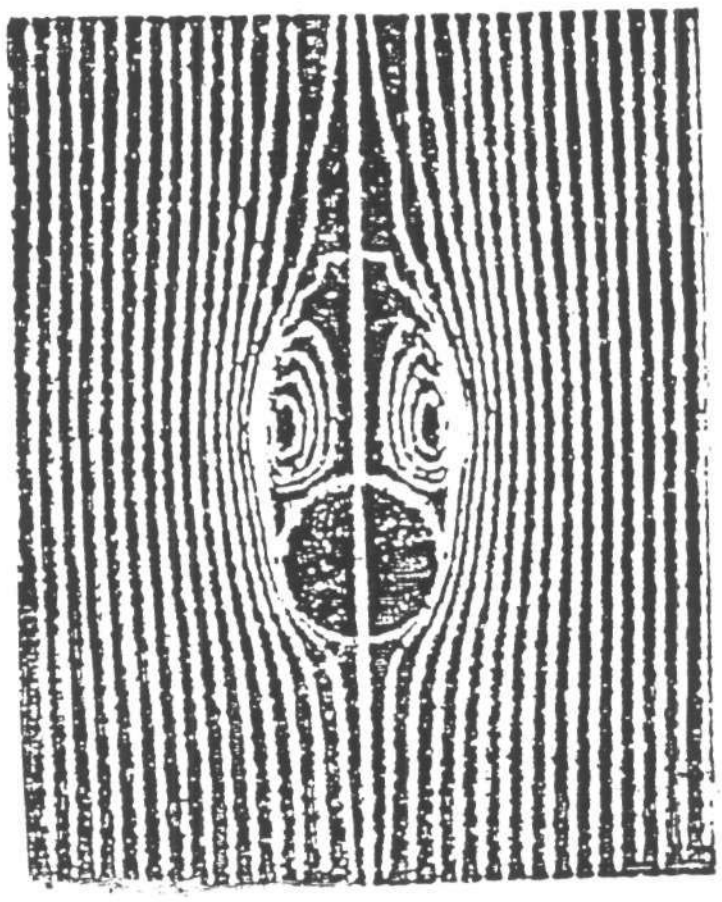


FIGURE 3.1: STREAM LINES AROUND A FALLING SPHERE(26)

Using the reduced variables,

$$\begin{aligned} T^* &= (T-T_o)/(T_\infty-T_o) \\ r^* &= r / R \\ \tau^* &= \alpha t / R^2 \\ U^*_\Theta &= RU_\Theta / \alpha \\ U^*_r &= RU_r / \alpha \\ \alpha &= k / \rho C_p \end{aligned} \tag{3.4}$$

We can write Eq. 3.2 in non-dimensional form (after dropping the stars) as

$$\frac{\partial T}{\partial \tau} + U_r \frac{\partial T}{\partial r} + \frac{U_\Theta}{r} \frac{\partial T}{\partial \Theta} = \frac{1}{r^2} \frac{\partial}{\partial r}\left(r^2 \frac{\partial T}{\partial r}\right) + \frac{1}{r^2 \sin\Theta} \frac{\partial}{\partial \Theta}\left(\sin\Theta \frac{\partial T}{\partial \Theta}\right). \tag{3.5}$$

The vapor mass diffusion equation can be obtained from Eq. 3.5 by replacing the dimensionless T by the corresponding dimensionless mass concentration C and the thermal diffusivity α by the diffusion coefficient D . Since the initial and boundary conditions necessary for solving these two equations are also similar, there is analogy between heat and mass tansfer.

The initial and boundary conditions for Eq. 3.5 are

$$\begin{aligned} &t = 0 \quad T = 0 \quad \text{at } r = 1 \quad \text{for all } \Theta \\ &\qquad T = 1 \quad \text{at } r > 1 \quad \text{for all } \Theta \\ &t > 0 \quad \frac{\partial T}{\partial \Theta} = 0 \quad \text{at } \Theta = 0, \pi \quad \text{for all } r \end{aligned} \tag{3.6}$$

$$\frac{\partial T}{\partial r} = 0 \qquad \text{for } r \to \infty \text{ and for all } \Theta$$

at r=1 (interface), the energy balance condition becomes

$$m_d c_p \frac{\partial T}{\partial t} = A_d \left[K_T \frac{\partial T}{\partial r} + h_{fg} D_T \frac{\partial \rho}{\partial r} \right] \tag{3.7}$$

3.4 COMBINED MOLECULAR AND TURBULENT (EDDY) DIFFUSION

The speed of fall in a steam-air atmosphere of droplets larger than 100 microns in diameter is great enough to develop eddies in the wake of such particles so that the mass transfer is accomplished not only by convection and molecular diffusion but also by bodily transport in fluid vortices, called turbulent diffusion. Turbulence is an irregular motion which in general makes its appearance in fluids when they flow past droplets. Since turbulent fluid motion is such a random fluid motion, a basic characteristic of turbulent flow is its duffusive action; accordingly, the exchange process is greater in turbulent than in non-turbulent flow. The diffusive action of turbulence is considered to result in an eddy viscosity or eddy heat conductivity from which the distribution of mean values can be calculated, just as in the kinetic theory of gases, where molecular transport processes result in a viscosity and heat conductivity.

We will start from the transport equation, where Prandtl tried to connect the coefficients of eddy diffusion ε_m and ε_h with the characteristics of the turbulence. According to the kinetic theory of

gases, the kinematic viscosity is equal to the product of a mixing-length and some suitable velocity. The mixing-length theory arose out of early attempts by Prandtl to describe turbulent flow quantitatively. It was well known that the friction loss occurring during turbulent flow was many times that attributable to molecular viscosity alone.

Combining the turbulent diffusion with that of molecular, the total rate of mass transfer becomes

$$\frac{\dot{m}}{A} = -(D_m + \varepsilon_m)\frac{d\rho}{dr} \qquad (3.8)$$

where ε_m is the eddy diffusivity of momentum. Similarly for heat transfer, we have

$$\frac{\dot{q}}{\rho_s c_p A} = -(\alpha + \varepsilon_h)\frac{dT}{dr} \qquad (3.9)$$

or

$$\frac{\dot{q}}{A} = -K_T \frac{dT}{dr} \qquad (3.10)$$

where ε_h = eddy diffusivity of heat,

and K_T is the total conductivity which is made up of the molecular conductivity and the eddy conductivity of heat,

$$K_T = K_m + K_t$$

However, $\varepsilon_m=\varepsilon_h=V_t$, which is the eddy viscosity, and this resulted from the various assumptions Prandtl made in the analysis. He assumed that the mixing-length for heat transfer is the same as the mixing-length for momentum transfer; that is, a particle of fluid travels the same distance before losing its identity and before attaining a different temperature.

The molecular diffusivities of a fluid are related by the Prandtl and Schmidt numbers:

$$Pr = \frac{V}{\alpha} = \frac{C_p \mu}{k} \tag{3.11}$$

$$Sc = \frac{V}{D_m} = \frac{\mu}{\rho D_m} \tag{3.12}$$

These are properties of the fluid and diffusing substance. Similarly, turbulent Prandtl and Schmidt numbers are

$$Pr_t = \frac{V_t}{\alpha_t}$$

$$Sc_t = \frac{V_t}{D_t}$$

These are properties of the flow and of position in it, as well as of the fluid and diffusing substance. In fully turbulent regions, they characterize the diffusive activity more closely than do their molecular counterparts. The molecular values vary over wide ranges and for

liquids the Prandtl and Schmidt numbers are strongly dependent on temperature. In a full turbulent flow, however, the mechanisms of transport are much the same for momentum and energy; admittedly mediated by molecular diffusion. Hence the ratios of the effective diffusivites differ only a little from unity for a wide range of flows and fluids. A much used approach to turbulent diffusion (which is applied in this study) is through the assumptions:

$$Pr_t = Sc_t = 1 \tag{3.13}$$

From this, we have

$$\alpha_t = D_t = V_t$$

and

$$K_t = \rho_\infty c_p V_t$$

V_t is given by an experimental correlation due to Smagorinsky (33) as

$$V_t = (c_1 \lambda^*)^2 \sqrt{\left(\frac{\Phi}{\mu}\right)} \tag{3.14}$$

where $c_1 = 0.2$, $\lambda^* = d$ and Φ is the dissipation function given by

$$\Phi = \frac{\mu}{2}\left[2\left(\varepsilon_{rr}^2 + \varepsilon_{\theta\theta}^2 + \varepsilon_{\phi\phi}^2\right) + \varepsilon_{\theta\phi}^2 + \varepsilon_{\theta r}^2 + \varepsilon_{r\phi}^2\right]$$

where in two dimensional spherical coordinate system (r, θ) since the analysis is independent of ϕ, we have

$$\varepsilon_{r\phi} = \varepsilon_{\theta\phi} = 0$$

$$\varepsilon_{\phi\phi} = \frac{U_r}{r} + \frac{U_\theta \mathrm{Cot}\theta}{r}$$

$$\varepsilon_{\theta r} = r \frac{\partial}{\partial r}\left(\frac{U_\theta}{r}\right) + \frac{1}{r}\frac{\partial U_r}{\partial \theta} \qquad (3.15)$$

$$\varepsilon_{rr} = \frac{\partial U_r}{\partial r}$$

$$\varepsilon_{\theta\theta} = \frac{1}{r}\frac{\partial U_\theta}{\partial \theta} + \frac{U_r}{r}$$

TOTAL DIFFUSIVITY, D_T

The total diffusivity, D_T (molecular plus turbulent) is defined as

$$D_T = D_m + D_t \qquad (3.16)$$

here, D_m is the molecular diffusivity of steam in air and D_t has been defined as the turbulent diffusivity. The following correlation was used to calculate the D_m(10):

For T >400K

$$D_m \ (\mathrm{cm}^2/\mathrm{s}) = 5.385 \times 10^{-6} \ T^{1.88} \ . \qquad (3.17)$$

Thus, the total diffusivity was reduced to a distribution around the droplet and kept constant for the program. $D_T(r,\theta) = D_m + D_t(r,\theta)$. Table 5.8 gives the distribution of the turbulent diffusivity.

3.5 DENSITY OF AIR IN MIXTURE:

The density of the air in the mixture was obtained by applying the equation of state of an ideal gas:

$$\rho_a = \frac{P_a}{R\,T_a} \qquad (3.18)$$

A semi-empirical relation gives the partial pressure of air to be

$$P_a(\text{atm}) = \frac{T}{298.16} \qquad T \text{ in } ^\circ K \tag{3.19}$$

When these relations are used, a fairly constant value of the air density is obtained for the mixture temperature equal or greater than 400K. Thus the value of the air density was taken constant for the whole flow region. When computed for $T_a = 403.16^\circ K$, we have

$$\rho_a = 0.001185 \text{ gm/cm}^3$$

DENSITY OF VAPOR IN MIXTURE:

The density distribution of the vapor was updated at the end of each time step by the use of the following correlation (21):

$$\rho_s = \frac{P_s(T)}{RT} \tag{3.20}$$

where $P_s(T) = 6.0573 \times 10^{26} T^{-5.3512} e^{-6890.81/T}$ N/m^2, T in $^\circ$K

and $R = 485.27 - 0.07966T$ J/K$_g$mole $^\circ$K

For example, at T = 353.15K, we obtained

$$\rho_s(\text{Eq. 3.20}) = 0.2921 \times 10^{-3} \text{ gm/cm}^3$$

$$\rho_s(\text{exact}) = 0.2925 \times 10^{-3} \text{ gm/cm}^3$$

This is the equation used for the boundary condition at the droplet surface; making use of the new droplet surface temperature distribution each time to compute the new density distribution, $\rho_s(r,\theta)$.

DENSITY OF MIXTURE:

$$\rho_m = x_s\rho_s + x_a\rho_a \tag{3.21}$$

This was the density taken as that of the atmosphere (ρ_∞); x_s,x_a are the mole fractions of air and steam in the mixture respectively. Actually, the effect of the air in mixture came into play only in the overall density of the atmosphere and the molecular diffusivity of steam in air, D_m.

CHAPTER 4

NUMERICAL COMPUTATION

The dimensionless energy equation and the set of boundary conditions presented in Chapter 3 are solved numerically. The first step in the solution of the equation by a finite difference method is to reduce it from continuous to discrete form, and then to solve the resulting algebraic equation on a digital computer. The basic method is to expand the terms of the original partial differential equation in Taylor's series. The series are truncated to a reasonble accuracy and a finite-difference equation is obtained by the replacement of each term by the truncated series. Each finite-difference equation relates the value of a function at any mesh point to the values at neighboring mesh points. In the present work, a five point approximation, involving four neighboring points, has been used (25, 27, 34). The domain over which the equation is to be integrated, the flow region, is represented by a finite number of points spaced systematically within the domain. The mesh points are spaced uniformly in both the r and θ-directions along with the assumption that the flow around the vertical axis is axisymmetric, and all variables are independent of ϕ.

4.1 Numerical Solution Procedure

Rearranging the governing energy equation from Chapter 3, we have,

$$\frac{\partial T}{\partial \tau} = \frac{\partial^2 T}{\partial r^2} + \left(\frac{2}{r} - U_r\right)\frac{\partial T}{\partial r} + \left(\frac{\cot\theta}{r^2} - \frac{U_\theta}{r}\right)\frac{\partial T}{\partial \theta} + \frac{1}{r^2}\frac{\partial^2 T}{\partial \theta^2} \qquad (4.1)$$

We introduce a mesh of points in a cross-sectional plane for which the azimuthal angle ϕ is constant; the mesh is defined as shown in Fig. 4.1, by the intersection of the curves

$$r_i = 1+(n+1-i)\Delta r;\ \theta_j = j\Delta\theta \qquad (4.2)$$

n is the number of mesh points in the radial direction.

An approximate relation between the temperature $T_{i,j}^{k+1}$ at a time step k+1 and $T_{i,j}^{k}$ along with its four nearest neighboring points $T_{i+1,j}^{k}$, $T_{i-1,j}^{k}$, $T_{i,j+1}^{k}$ and $T_{i,j-1}^{k}$ at a time step k, and at an arbitrary mesh point ($r_i = i\Delta r$, $\theta_j = j\Delta\theta$) can be obtained by expanding T in a Taylor's series about the point (i, j, k) keeping only terms to second order:

$$T(r,\theta,\tau)=T(r_i,\theta_j,\tau_k) + \left.\frac{\partial T}{\partial r}\right|_{i,j,k}(r-r_i) + \left.\frac{\partial^2 T}{\partial r^2}\right|_{i,j,k}\frac{(r-r_i)^2}{2} + \left.\frac{\partial T}{\partial \theta}\right|_{i,j,k}(\theta-\theta_j)$$

$$+ \left.\frac{\partial^2 T}{\partial \theta^2}\right|_{i,j,k}\frac{(\theta-\theta_j)^2}{2} + \left.\frac{\partial T}{\partial \tau}\right|_{i,j,k}(\tau-\tau_k)+\cdots \qquad (4.3)$$

By setting r and θ successively equal to $(i\pm1)\Delta r$ and $(j\pm1)\Delta\theta$, Eq. 4.3 gives rise to four expressions relating $T_{i,j}^{k}$ and $T_{i\pm1,\,j\pm1}^{k}$ to the derivatives of T at (i, j, k). That is,

$$T(r_i+\Delta r,\theta_j,\tau_k) - T(r_i,\theta_j,\tau_k) = \frac{\partial T}{\partial r}\bigg|_{i,j,k} \Delta r + \frac{\partial^2 T}{\partial r^2}\bigg|_{i,j,k} \frac{(\Delta r)^2}{2} \quad (4.4)$$

$$T(r_i-\Delta r,\theta_j,\tau_k) - T(r_i,\theta_j,\tau_k) = -\frac{\partial T}{\partial r}\bigg|_{i,j,k} \Delta r + \frac{\partial^2 T}{\partial r^2}\bigg|_{i,j,k} \frac{(\Delta r)^2}{2} \quad (4.5)$$

$$T(r_i,\theta_j+\Delta\theta,\tau_k)-T(r_i,\theta_j,\tau_k) = \frac{\partial T}{\partial \theta}\bigg|_{i,j,k} \Delta\theta + \frac{\partial^2 T}{\partial \theta^2}\bigg|_{i,j,k} \frac{(\Delta\theta)^2}{2} \quad (4.6)$$

$$T(r_i,\theta_j-\Delta\theta,\tau_k)-T(r_i,\theta_j,\tau_k) = -\frac{\partial T}{\partial \theta}\bigg|_{i,j,k} \Delta\theta + \frac{\partial^2 T}{\partial \theta^2}\bigg|_{i,j,k} \frac{(\Delta\theta)^2}{2} \quad (4.7)$$

and by setting τ equal to $(k+1)\Delta\tau$, we have

$$T(r_i,\theta_j,\tau_k+\Delta\tau) - T(r_i,\theta_j,\tau_k) = \frac{\partial T}{\partial \tau}\bigg|_{i,j,k} \Delta\tau \quad (4.8)$$

These five equations, together with the differential Eq. 4.1 allows us to eliminate the derivatives in Eq. 4.3 and thus to obtain an equation relating $T^{k+1}_{i,j}$ to $T^{k}_{i,j}$ and $T^{k}_{i\pm1,j\pm1}$ in terms of the known quantities such as r_i and $\cot\theta_j$:

$$T^{k+1}_{i,j} = A_{ij}T^{k}_{i+1,j} + B_{ij}T^{k}_{i-1,j} + G_i T^{k}_{i,j} + E_{ij}T^{k}_{i,j-1} + F_{ij}T^{k}_{i,j+1} \quad (4.9)$$

where

$$A_{ij} = \frac{\Delta\tau}{(\Delta r)^2} + \frac{\Delta\tau}{2\Delta r}\left(\frac{2}{r_i} - U_{rij}\right) \quad (4.9.1)$$

$$B_{ij} = \frac{\Delta\tau}{(\Delta r)^2} - \frac{\Delta\tau}{2\Delta r}\left(\frac{2}{r_i} - U_{rij}\right) \quad (4.9.2)$$

$$G_i = 1 - \frac{2\Delta\tau}{(\Delta r)^2} - \frac{2\Delta\tau}{r_i^2(\Delta\theta)^2} \tag{4.9.3}$$

$$E_{ij} = \frac{\Delta\tau}{r_i^2(\Delta\theta)^2} - \frac{\Delta\tau}{2\Delta\theta}\left(\frac{\cot\theta_j}{r_i^2} - \frac{U_{\theta ij}}{r_i}\right) \tag{4.9.4}$$

$$F_{ij} = \frac{\Delta\tau}{r_i^2(\Delta\theta)^2} + \frac{\Delta\tau}{2\Delta\theta}\left(\frac{\cot\theta_j}{r_i^2} - \frac{U_{\theta ij}}{r_i}\right) \tag{4.9.5}$$

From the derived finite-difference equation, it follows that the diffusion term and the non-linear convective term have been approximated by a central difference scheme, which is second order accurate. On the other hand, the time dependence of the temperature has been approximated by the forward difference scheme. Here, i,j are used to denote the location in r and θ directions respectively, and k represents the number of time steps. For convergence of the solution, the criterion used is

$$\Delta\tau\left(\frac{1}{(\Delta r)^2} + \frac{1}{(r\Delta\theta)^2}\right) < 1/2 \tag{4.10}$$

The Courant criterion $\left(\frac{U_t\Delta t}{\Delta r} < 1\right)$, for convergence taking into account the convective term of the energy equation has been tested and found to be greater than the dimensionless time increment for the diffusive term. As such, the inequality 4.10 is used for this study.

4.2 Boundary Conditions

We have chosen an approximation to the physical geometry of the falling droplet by constructing the boundaries with two types of boundary segments. In a cross-sectional plane (ϕ=constant) regions consist of straight line segments and arcs of circles, all concentric with the surface of the droplet. The volume in which the energy equation is to be solved must be completely enclosed by boundaries made up of such segments. The segments are identified by the order in which they occur as θ increases from 0 to π, and each boundary segment is specified by its type (line or circle), the constants of its equation in polar coordinates, and the largest value of θ for that segment. The mesh, the initial approximations to temperature at each mesh point, the distances between neighboring mesh points, and the boundaries are set up automatically after the equation and temperatures of the boundary segments and the desired mesh spacings (Δr and $\Delta\theta$) have been specified.

When the point (i,j) is on the θ=0 or π axis, the last term in Eq. 4.1 vanishes because $\partial T/\partial\theta=0$ for these values of θ. By carrying out the procedure described in the numerical solution procedure section, relations for this case are given below:

$$T_{i,1}^{k+1} = A_{i1}T_{i+1,1}^{k} + B_{i1}T_{i-1,1}^{k} + D_i T_{i,1}^{k} + \frac{\Delta\tau}{2r_i^2(\Delta\theta)^2}T_{i3}^{k} \qquad (4.11)$$

$$T_{i,m+1}^{k+1} = A_{i,m+1}T_{i+1,m+1}^{k} + B_{i,m+1}T_{i-1,m+1}^{k} + D_i T_{i,m+1}^{k} + \frac{\Delta\tau}{2r_i^2(\Delta\theta)^2}T_{i,m-1}^{k}$$

m is the number of mesh points in the angular direction.

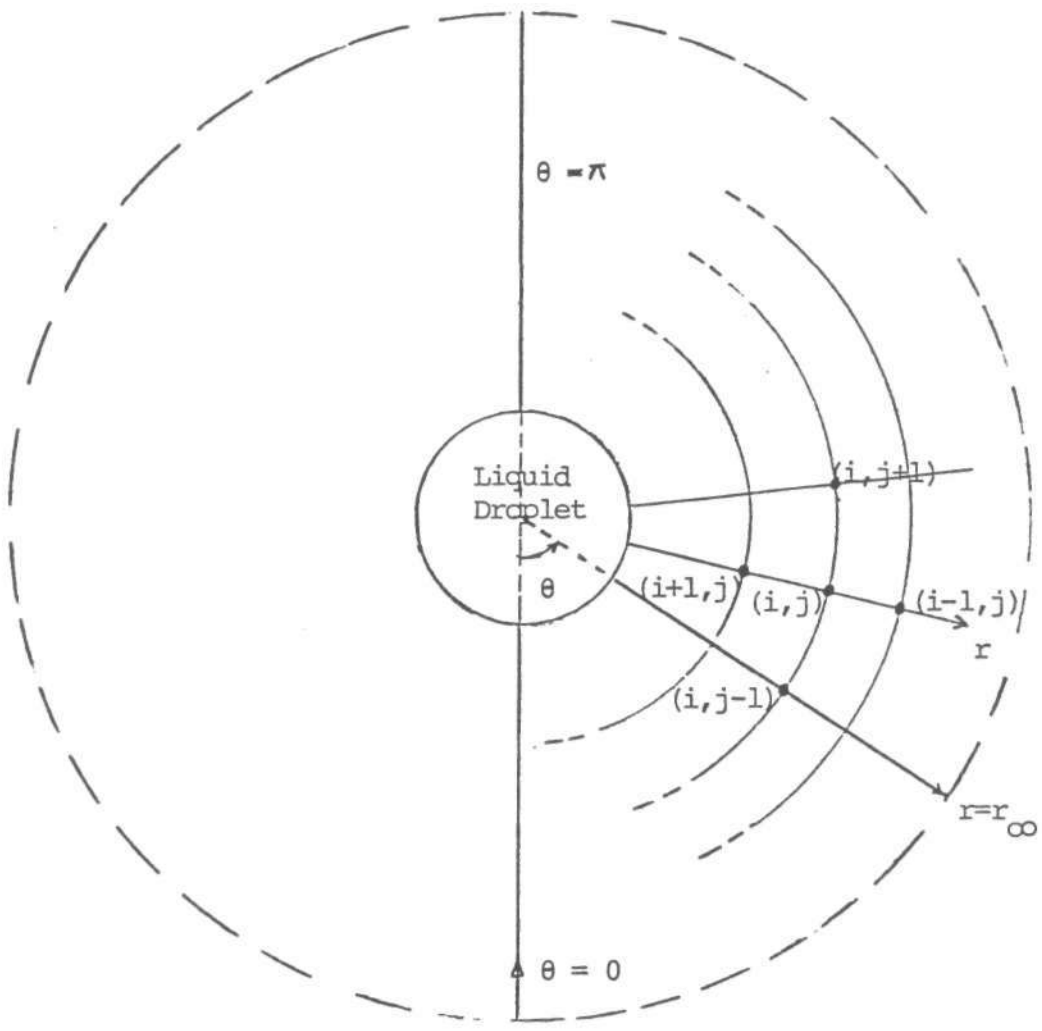


Figure 4.1 Schematic diagram of the circular mesh system.

$$\text{where } D_i = \left[1 - \frac{2\Delta\tau}{(\Delta r)^2} - \frac{\Delta\tau}{2r_i^2(\Delta\theta)^2}\right] \tag{4.11a}$$

At far distance from the droplet surface, we have the condition

$$T_{1j}^{k+1} = 1.0 \tag{4.12}$$

and the surface boundary condition is obtained from a heat balance as follows:

$$m_d c_p \frac{dT}{dt} = 2\pi R^2 \sum_j \dot{q}''(\theta_j)\left[\cos\left(\theta_j - \frac{\Delta\theta}{2}\right) - \cos\left(\theta_j + \frac{\Delta\theta}{2}\right)\right] \tag{4.13}$$

where

$$\dot{q}'' = K_T \frac{\partial T}{\partial r} + h_{fg} D_T \frac{\partial \rho}{\partial r} \tag{4.13a}$$

In Eq. 4.13a, the first term on the right accounts for the conduction of heat into the droplet, the second for the condensation on the droplet. All these equations are transformed into FORTRAN language for the purpose of running the program. The flow chart and the list of this program are shown in Appendices A, B, and C.

CHAPTER 5

5.1 DISCUSSION OF RESULTS

The cooling of the atmosphere by a falling water droplet was calculated according to the complete mixing model. The accuracy of the results obtained and the economy of the procedure used, like any other finite difference method, are dependent on the mesh sizes, magnitude of the time step, position of the outer boundary, and convergence criteria. Values of these factors were found on the basis of numerical methods and were selected in order to achieve convergence. In the present study, the values of the mesh constants Δr, $\Delta\theta$, $\Delta\tau$ used in the program are set equal to 0.1, 6° and 0.0026, respectively.

The problem was programmed in FORTRAN IV (Appendices B and C) and run on an IBM computer. The results of the calculation are summarized in Tables 5.3 - 5.5, plotted in Figures 5.1-5.4, and given in complete form in Tables 5.9 - 5.19 for the temperature and density distributions. Fig. 5.2 shows the plot for the two heat fluxes (condensing and sensible) and the total heat flux. It can be seen that the condensing part of the total heat flux dominates the transfer process.

5.2 HEAT TRANSFER COEFFICIENT(h)

The overall heat transfer coefficient to the droplet is defined by the relationship

$$h = \frac{\dot{Q}''_s}{\Delta T} \quad \text{cal / cm}^2\text{s°K}, \tag{5.1}$$

$\dot{Q}"_s$ is the sensible heat flux and ΔT is the temperature difference between the droplet surface and the bulk of the air-steam mixture. In dimensionless temperature form, we have

$$\frac{\dot{Q}"_s}{\Delta T} = h \frac{(T_\infty - T)}{(T_\infty - T_o)} \tag{5.2}$$

T is the variable droplet surface temperature.

Since $T_s = \frac{(T-T_o)}{(T_\infty - T_o)}$, we have

$$1-T_s = \frac{(T_\infty - T)}{(T_\infty - T_o)}$$

where T_s is the dimensionless droplet surface temperature. Thus,

$$\frac{\dot{Q}"_s}{\Delta T} = h(1-T_s) \tag{5.3}$$

Fig. 5.2 gives the plot of $\frac{\dot{Q}"_s}{\Delta T}$ against $(1-T_s)$. When these data are fitted into a polynominal of the third order, the following relationship is obtained:

$$F(x) = C_o + C_1 x + C_2 x^2 + C_3 x^3 \tag{5.4}$$

where $F = \frac{\dot{Q}"_s}{\Delta T}$, $x = 1-T_s$,

$C_o = -5.2902933$,

$C_1 = 18.8827631$,

$C_2 = -22.4382146$, and

$C_3 = 8.885428$.

Differentiating Eq. 5.4 gives the heat transfer coefficient, h, as a function of x as

$$h(x) = C_1 + 2C_2x + 3C_3x^2 \qquad (5.5)$$

The average heat transfer coefficient during the droplet transit $\langle h \rangle$ is given as

$$\langle h \rangle = \frac{\int h(x)dx}{\int dx} \qquad (5.6)$$

Substituting Eq. 5.5 into Eq. 5.6 and evaluating the integral within the range $0.7409 < x < 0.9333$, we have

$$\langle h \rangle = 0.078 \text{ cal/cm}^2\text{s°K}$$

Table 5.2 gives the theoretical value of the heat transfer coefficient. The value computed in this study agreed fairly well with this value.

5.3 MASS TRANSFER COEFFICIENT (k_g)

In an analogous way, the overall mass transfer coefficient is defined by the relationship,

$$\frac{\dot{m}''}{\Delta\rho} = k_g (1-C_s) \qquad (5.7)$$

where $\dot{m}''$ is the mass flux and $\Delta\rho$ is the concentration difference in g/cm^3 of the transferred material between the bulk of the surrounding fluid and the surface of the droplet; C_s is the dimensionless droplet surface concentration. Fig. 5.3 gives the plot of $\frac{\dot{m}''}{\Delta\rho}$ against $(1-C_s)$. However, when these data are fitted into a polynomial of the third order, the following relationship is obtained:

$$f(y) = A_0 + A_1 y + A_2 y^2 + A_3 y^3, \tag{5.8}$$

where $f = \frac{\dot{m}''}{\Delta\rho}$ and $y = 1 - C_s$,

$A_0 = -6773.4624927,$

$A_1 = 23427.4104069,$

$A_2 = -27029.864832,$ and

$A_3 = 10405.1423465.$

Differentiating Eq. 5.8 gives the mass transfer coefficient, k_g, as a function of y, as

$$K_g(y) = A_1 + 2A_2 y + 3A_3 y^2. \tag{5.9}$$

The average mass transfer coefficient , $\langle k_g \rangle$ in an analogous way is given as

$$\langle k_g \rangle = \frac{\int k_g(y)dy}{\int dy} \tag{5.10}$$

Substituting Eq. 5.9 into Eq. 5.10 and evaluating the integral within the integral within the range 0.8353 <y>0.9655, we have the result

$\langle k_g \rangle = 103.103$ cm/s.

TABLE 5.1

TYPICAL PROGRAM RUN

INPUT DATA

STEAM TEMPERATURE, T∞	=130°C
DROPLET INITIAL TEMPERATURE	= 80°C
DROPLET DIAMETER, d	= 3mm.

TABLE 5.2

THEORETICAL MEAN HEAT-TRANSFER COEFFICIENTS

FOR VARIOUS DROP DIAMETER(2)

d (mm)	1.0	1.5	3.0	4.8	6.3
h,caL/cm^2sec°c	0.157	0.099	0.049	0.033	0.025

TABLE 5.3

SUMMARY OF RESULTS FROM COMPUTER RUNS

TIME HISTORY OF DIMENSIONLESS DROPLET TEMPERATURE AND DENSITY

Time (sec)	Temperature (T_s)	Density (C_s)
0.3553	0.0667	0.0345
0.7106	0.0953	0.0522
1 0659	0.1149	0.0645
1.4212	0.1299	0.0741
1.7765	0.1421	0.0820
2.1317	0.1523	0.0887
2.4870	0.1611	0.0946
2.8423	0.1688	0.0998
3.1976	0.1757	0.1045
3.5529	0.1818	0.1087
3.9082	0.1874	0.1125
4.2635	0.1925	0.1161
4.6188	0.1972	0.1194
4.974	0.2015	0.1224
5.3293	0.2055	0.1252
5.6846	0.2092	0.1279
6.0399	0.2127	0.1304
6.3952	0.2160	0.1327
6.7505	0.2191	0.1350
7.1058	0.2220	0.1371
8.5269	0 2322	0.1445
9.9481	0.2406	0.1507
11.3692	0.2477	0.1560
12.7900	0.2538	0.1607
14.212	0.2591	0.1647

TABLE 5.4

TIME HISTORY OF HEAT AND MASS FLUXES TO DROPLET

Time (sec)	Total Heat Flux $\dot{Q}''_t$ (cal/cm^{2}s)	Condensing Heat Flux $\dot{Q}''_c$ (cal/cm^{2}s)	Sensible Heat Flux $\dot{Q}''_s$ (cal/cm^{2}s)	Mass Flux $\dot{m}''$ (g/cm^{2}s)
0.3553	8.170	7.400	0.770	0.0140
0.7106	4.950	4.500	0.450	0.0086
1.0659	3.520	3.200	0.320	0.0062
1.4212	2.750	2.500	0.250	0.0049
1.7765	2.300	2.100	0.200	0.0040
2.1317	1.970	1.800	0.170	0.0034
2.4870	1.640	1.500	0.140	0.0029
2.8423	1.430	1.300	0.130	0.0026
3.1976	1.310	1.200	0.110	0.0023
3.5529	1.200	1.100	0.100	0.0020
3.9082	1.060	0.970	0.090	0.0019
4.2635	0.962	0.880	0.082	0.0017
4.6188	0.885	0.810	0.075	0.0016
4.974	0.819	0.750	0.069	0.0014
5.3293	0.763	0.700	0.063	0.0013
5.6846	0.709	0.650	0.059	0.0012
6.0399	0.665	0.610	0.055	0.00116
6.3952	0.621	0.570	0.051	0.0011
6.7505	0.588	0.540	0.048	0.0010
7.1058	0.555	0.510	0.045	0.00098
8.5269	0.447	0.410	0.037	0.0008
9.9481	0.380	0.350	0.030	0.00067
11.3692	0.326	0.300	0.026	0.00057
12.790	0.282	0.260	0.022	0.0005
14.212	0.250	0.230	0.020	0.00044

TABLE 5.5

DATA FOR HEAT AND MASS TRANSFER COEFFICIENTS

$(1-T_s)$	$\dot{Q}''_s / \Delta T$ cal / cm2s K	$(1-C_s)$	$\dot{m}''_{cm} / \Delta\rho$ / s
0.9333	0.0154	0.9655	13.860
0.9050	0.0090	0.9478	8.515
0.8850	0.0064	0.9355	6.139
0.8700	0.0050	0.9259	4.850
0.8580	0.0040	0.9180	3.960
0.8480	0.0034	0.9113	3.366
0.8389	0.0028	0.9054	2.871
0.8312	0.0026	0.9002	2.574
0.8243	0.0022	0.8955	2.277
0.8182	0.0020	0.8913	1.980
0.8126	0.0018	0.8875	1.880
0.8075	0.00164	0.8839	1.683
0.8028	0.0015	0.8806	1.584
0.7985	0.00138	0.8776	1.386
0.7945	0.00126	0.8748	1.287
0.7908	0.00118	0.8721	1.188
0.7873	0.0011	0.8696	1.148
0.7840	0.00102	0.8673	1.089
0.7810	0.00096	0.8650	0.990
0.7780	0.0009	0.8629	0.970
0.7678	0.00074	0.8555	0.792
0.7594	0.0006	0.8493	0.663
0.7523	0.00052	0.8440	0.564
0.7462	0.00044	0.8393	0.495
0.7409	0.0004	0.8353	0.436

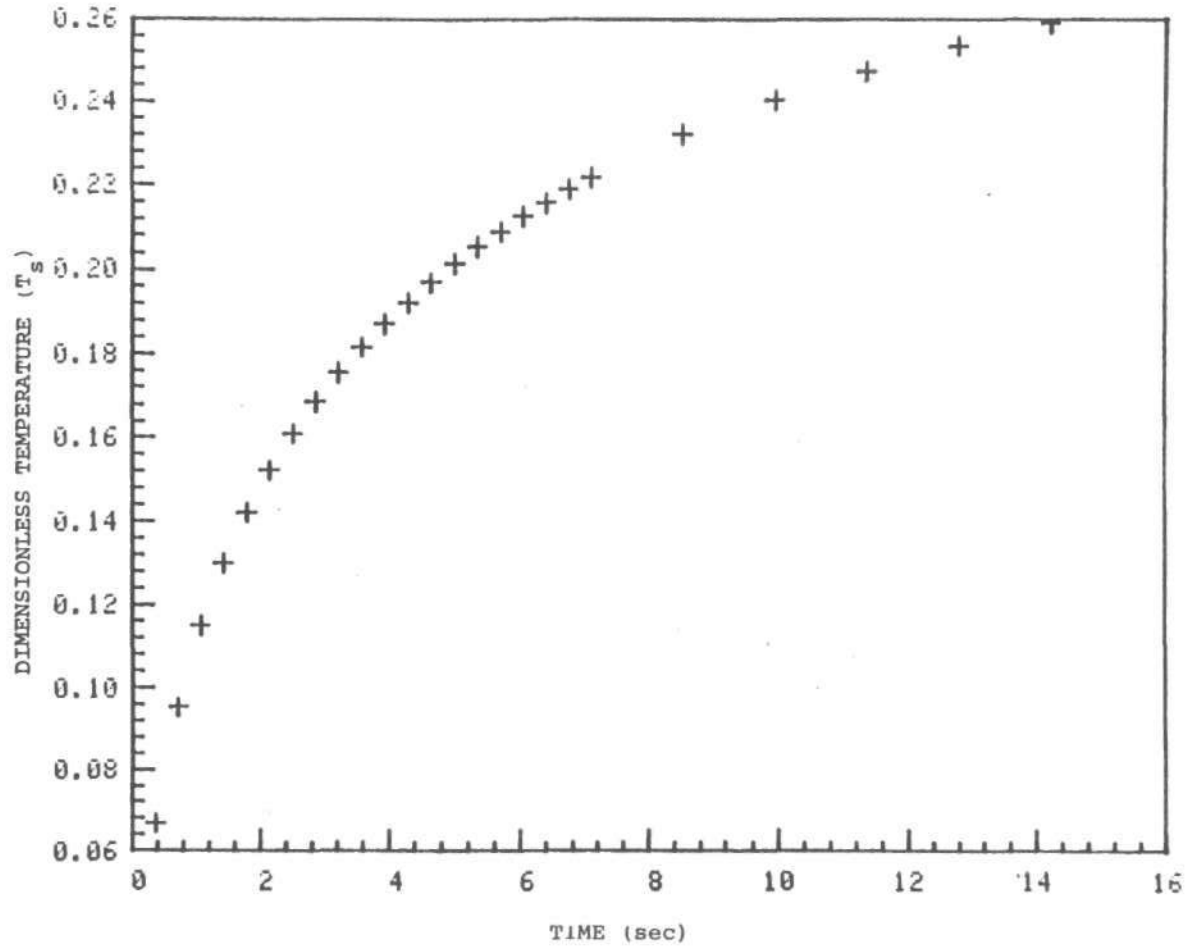


FIGURE 5.1: TEMPERATURE-TIME CHARACTERISTIC.

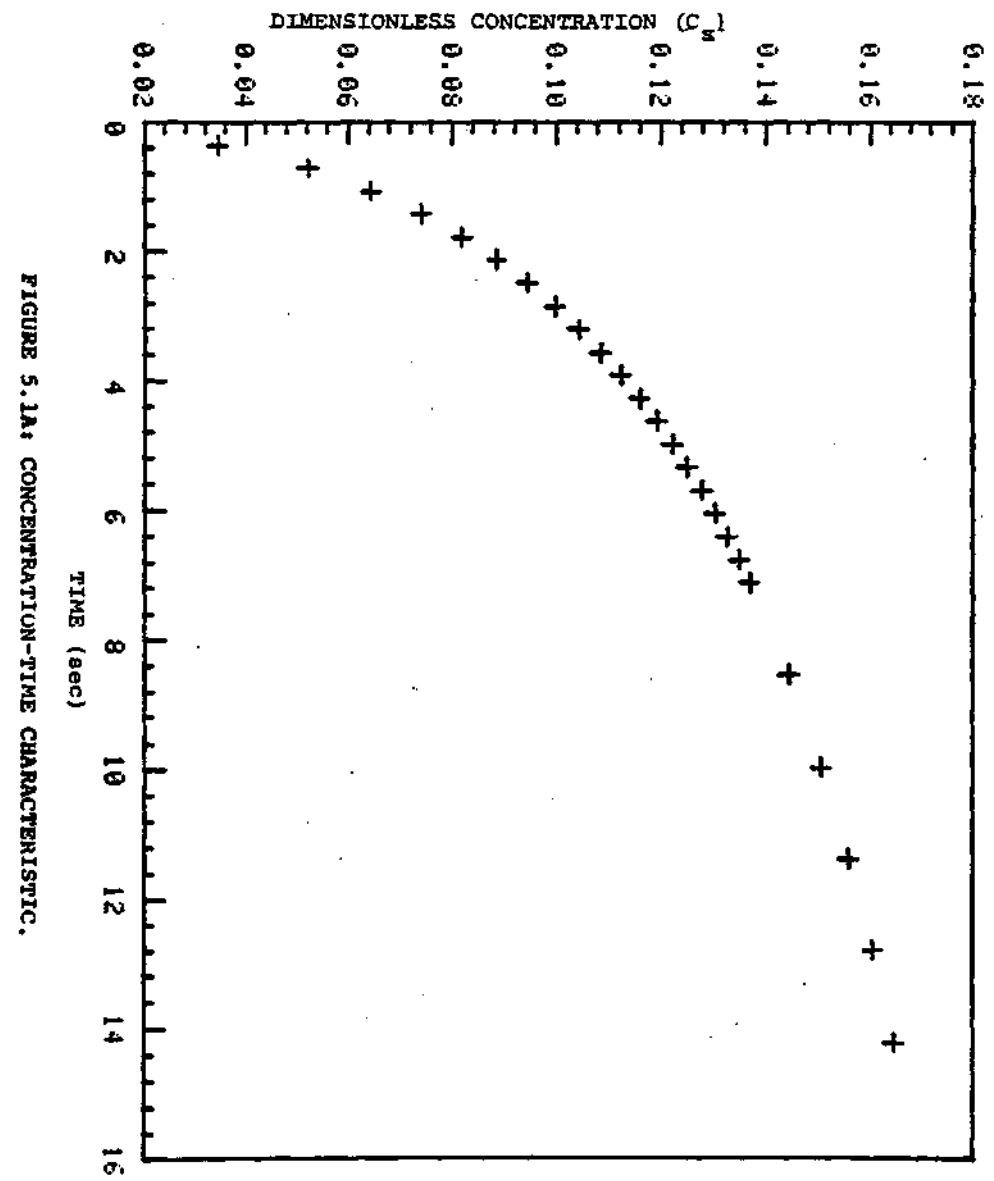


FIGURE 5.1A: CONCENTRATION-TIME CHARACTERISTIC.

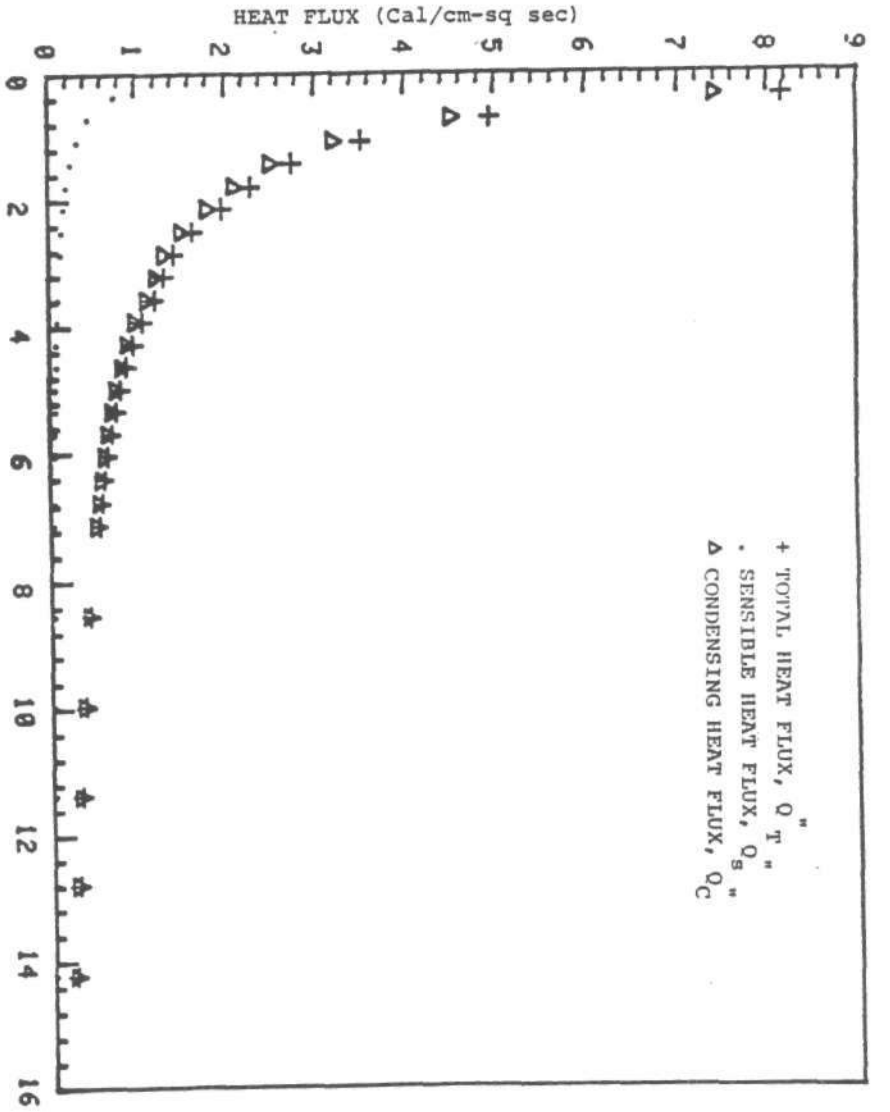
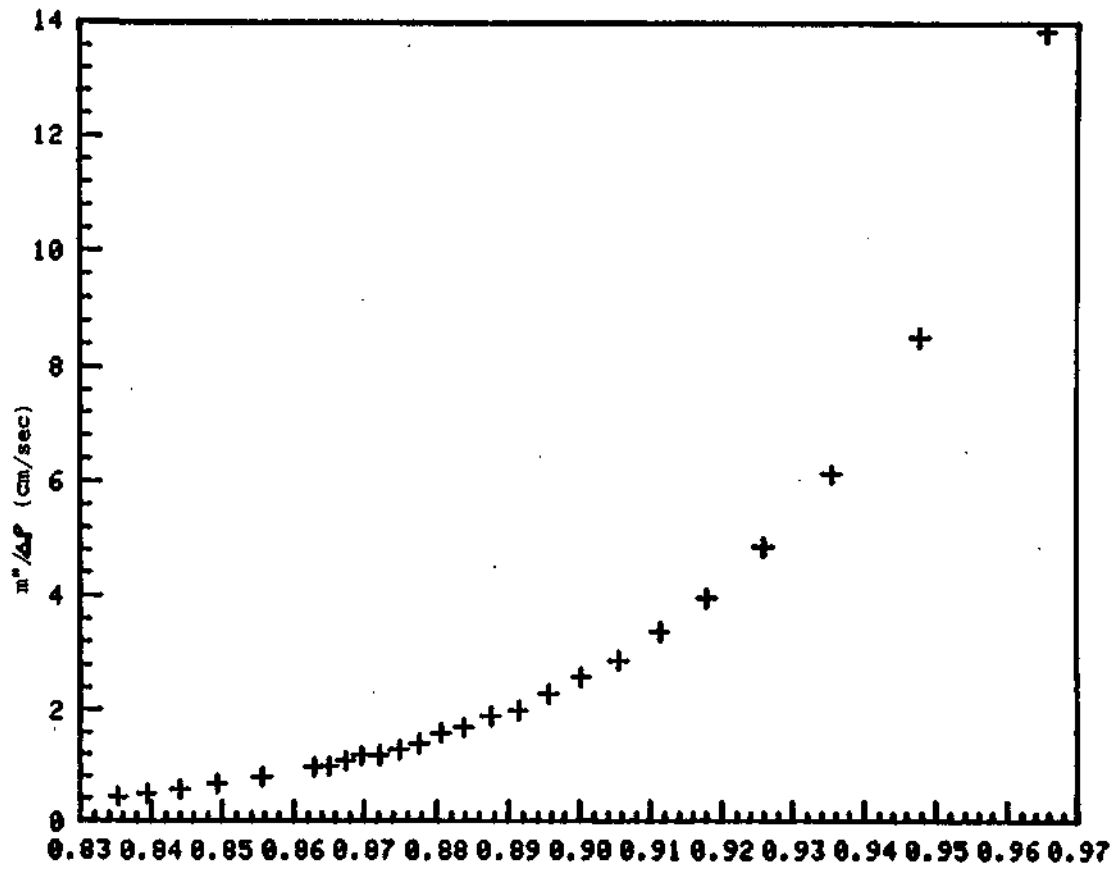


FIGURE 5.2: HEAT FLUX - TIME CHARACTERISTICS.



DIMENSIONLESS TEMPERATURE DIFFERENCE $(1-C_s)$

FIGURE 5.3: MASS TRANSFER COEFFICIENT CORRELATION.

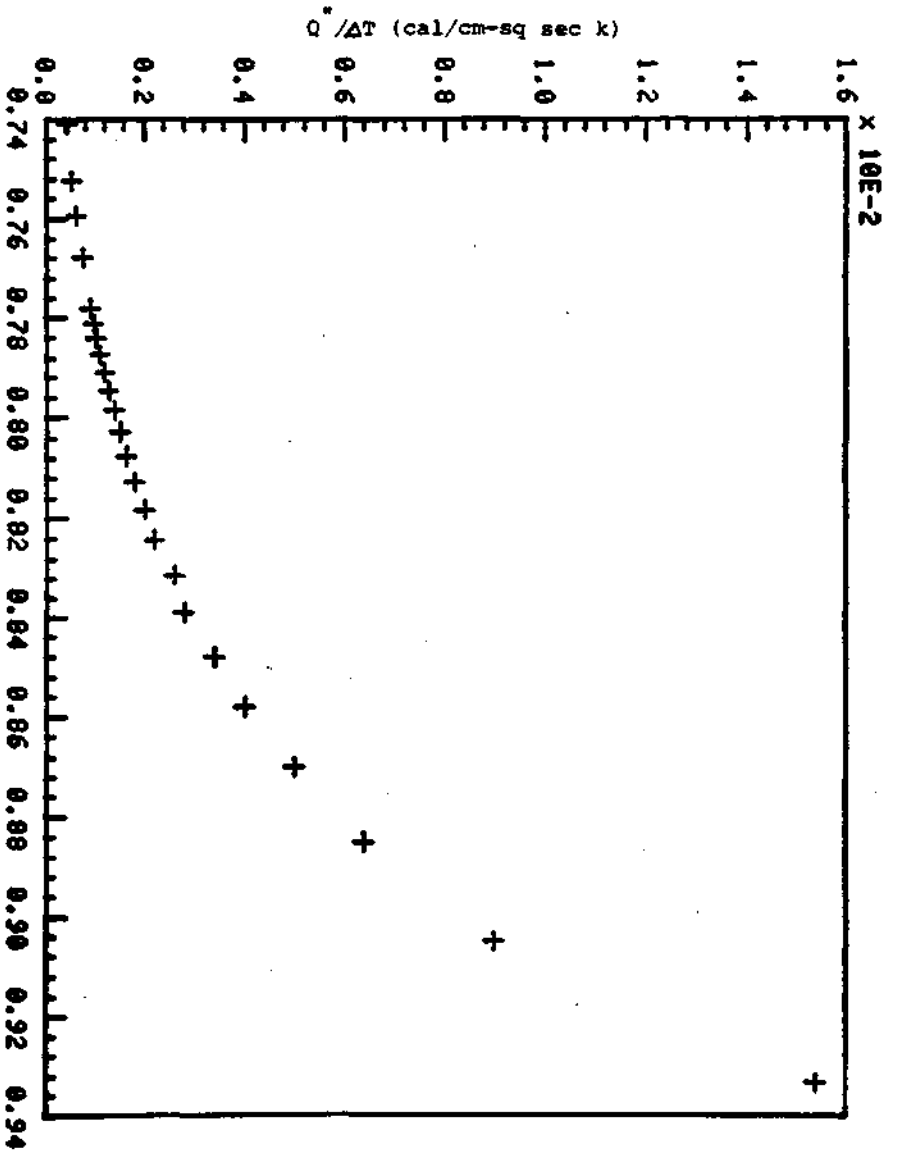


FIGURE 5.4: HEAT TRANSFER COEFFICIENT CORRELATION.

TABLE 5.6

RADIAL VELOCITY COMPONENT DISTRIBUTION

DIMENSIONLESS RADIUS

ANGLE	1.0	1.1	1.2	1.3	1.4	1.5	1.6	1.7	1.8	1.9	2.0
180	0.00	-2.82	-2.82	-2.82	-2.82	-2.82	-2.82	-2.82	-2.82	-2.82	-2.82
174	0.00	-0.59	-0.90	-0.87	-0.91	-0.92	-0.93	-0.93	-0.93	-0.91	-0.29
168	0.00	-0.24	-0.86	-0.79	-0.88	-0.90	-0.93	-0.93	-0.92	-0.89	0.37
162	0.00	-0.26	-0.73	-0.78	-0.87	-0.92	-0.91	-0.88	-0.81	0.55	0.51
156	0.00	-0.36	-0.59	-0.56	-0.79	-0.89	-0.90	0.26	0.70	0.70	0.80
150	0.00	-0.16	-0.35	-0.38	-0.47	0.81	0.80	0.71	0.70	0.77	0.87
144	0.00	-0.13	-0.12	-0.09	0.80	0.74	0.66	0.66	0.72	0.74	0.82
138	0.00	0.17	0.26	0.64	0.70	0.70	0.70	0.72	0.75	0.75	0.75
132	0.00	0.19	0.88	0.92	0.78	0.72	0.71	0.69	0.69	0.69	0.69
126	0.00	0.56	0.64	0.61	0.68	0.64	0.64	0.61	0.61	0.61	0.61
120	0.00	0.53	0.54	0.60	0.57	0.53	0.53	0.53	0.53	0.53	0.53
114	0.00	0.56	0.53	0.53	0.47	0.42	0.42	0.42	0.42	0.42	0.42
108	0.00	0.46	0.45	0.44	0.42	0.33	0.33	0.33	0.33	0.33	0.33
102	0.00	0.40	0.36	0.32	0.31	0.22	0.22	0.22	0.22	0.22	0.22
96	0.00	0.29	0.26	0.22	0.21	0.13	0.12	0.12	0.12	0.12	0.14
90	0.00	0.19	0.15	0.12	0.09	0.00	0.00	0.00	0.00	0.00	0.00
84	0.00	0.12	0.10	0.07	-0.02	-0.08	-0.08	-0.08	-0.08	-0.08	-0.08
78	0.00	0.00	-0.07	-0.10	-0.12	-0.18	-0.18	-0.18	-0.18	-0.18	-0.18
72	0.00	-0.10	-0.12	-0.14	-0.14	-0.29	-0.29	-0.28	-0.28	-0.29	-0.29
66	0.00	-0.13	-0.15	-0.22	-0.26	-0.38	-0.39	-0.39	-0.38	-0.38	-0.38
60	0.00	-0.13	-0.13	-0.25	-0.34	-0.48	-0.47	-0.47	-0.47	-0.48	-0.47
54	0.00	-0.23	-0.29	-0.35	-0.35	-0.56	-0.56	-0.57	-0.57	-0.57	-0.57
48	0.00	-0.27	-0.39	-0.39	-0.66	-0.66	-0.65	-0.65	-0.66	-0.66	-0.66
42	0.00	-0.30	-0.40	-0.71	-0.71	-0.73	-0.73	-0.73	-0.73	-0.73	-0.72
36	0.00	-0.37	-0.55	-0.55	-0.62	-0.79	-0.79	-0.79	-0.79	-0.79	-0.79
30	0.00	-0.38	-0.57	-0.57	-0.85	-0.85	-0.85	-0.86	-0.86	-0.86	-0.87
24	0.00	-0.44	-0.45	-0.70	-0.70	-0.91	-0.91	-0.91	-0.91	-0.91	-0.91
18	0.00	-0.64	-0.64	-0.88	-0.93	-0.93	-0.93	-0.93	-0.94	-0.94	-0.95
12	0.00	-0.89	-0.89	-0.89	-0.96	-0.96	-0.97	-0.99	-0.98	-0.98	-0.98
6	0.00	-0.96	-0.96	-0.99	-0.99	-0.99	-0.99	-0.99	-0.99	-0.99	-0.99
0	0.00	-1.00	-1.00	-1.00	-1.00	-1.00	-1.00	-1.00	-1.00	-1.00	-1.00

TABLE 5.7

ANGULAR VELOCITY COMPONENT DISTRIBUTION

DIMENSIONLESS RADIUS

ANGLE	1.0	1.1	1.2	1.3	1.4	1.5	1.6	1.7	1.8	1.9	2.0
180	0.00	0.00	0.00	0.00	0.00	0.00	0.00	0.00	0.00	0.00	0.00
174	0.00	-0.21	-0.19	-0.20	-0.16	-0.13	-0.10	-0.09	0.05	0.07	0.26
168	0.00	-0.41	-0.38	-0.39	-0.32	-0.27	-0.15	-0.13	0.08	0.14	0.53
162	0.00	-0.47	-0.44	-0.47	-0.35	0.15	0.13	0.19	0.26	0.65	0.72
156	0.00	-0.62	-0.59	-0.67	-0.50	-0.29	0.19	0.72	0.59	0.63	0.56
150	0.00	-0.44	-0.56	-0.38	-0.27	0.45	0.46	0.60	0.68	0.62	0.48
144	0.00	-0.52	-0.65	-0.53	0.50	0.58	0.66	0.70	0.67	0.65	0.57
138	0.00	-0.27	-0.18	-0.21	0.63	0.63	0.70	0.69	0.66	0.66	0.66
132	0.00	-0.12	-0.47	-0.39	0.63	0.72	0.71	0.72	0.72	0.72	0.72
126	0.00	-0.56	0.76	0.79	0.73	0.77	0.77	0.79	0.79	0.79	0.79
120	0.00	0.84	0.79	0.81	0.85	0.85	0.85	0.85	0.85	0.85	0.85
114	0.00	0.83	0.85	0.85	0.88	0.91	0.91	0.91	0.91	0.91	0.91
108	0.00	0.87	0.88	0.90	0.90	0.95	0.95	0.95	0.95	0.95	0.95
102	0.00	0.90	0.93	0.94	0.95	0.99	0.99	0.99	0.99	0.99	0.99
96	0.00	0.95	0.96	0.97	0.97	0.99	0.99	0.99	0.99	0.99	0.99
90	0.00	0.97	0.97	0.98	0.99	1.00	1.00	1.00	1.00	1.00	1.00
84	0.00	0.98	0.98	0.98	0.93	0.99	0.99	0.99	0.99	0.99	0.99
78	0.00	0.98	0.98	0.98	0.98	0.98	0.98	0.98	0.98	0.98	0.98
72	0.00	0.96	0.97	0.98	0.98	0.96	0.96	0.96	0.96	0.96	0.96
66	0.00	0.96	0.97	0.96	0.96	0.92	0.92	0.92	0.92	0.92	0.92
60	0.00	0.94	0.94	0.94	0.93	0.87	0.80	0.88	0.88	0.87	0.88
54	0.00	0.92	0.90	0.91	0.91	0.83	0.83	0.82	0.82	0.82	0.82
48	0.00	0.89	0.87	0.88	0.75	0.75	0.76	0.76	0.76	0.75	0.75
42	0.00	0.83	0.86	0.66	0.66	0.68	0.68	0.68	0.68	0.68	0.69
36	0.00	0.75	0.73	0.73	0.74	0.60	0.60	0.60	0.60	0.62	0.62
30	0.00	0.74	0.76	0.76	0.53	0.53	0.53	0.50	0.52	0.51	0.51
24	0.00	0.71	0.76	0.65	0.65	0.42	0.42	0.42	0.42	0.42	0.41
18	0.00	0.71	0.71	0.34	0.36	0.36	0.35	0.35	0.34	0.34	0.30
12	0.00	0.24	0.24	0.24	0.26	0.26	0.24	0.17	0.18	0.18	0.18
6	0.00	0.14	0.14	0.14	0.14	0.14	0.14	0.14	0.15	0.15	0.14
0	0.00	0.00	0.00	0.00	0.00	0.00	0.00	0.00	0.00	0.00	0.00

TABLE 5.8

TURBULENT DIFFUSIVITY DISTRIBUTION

DIMENSIONLESS RADIUS

ANGLE	1.0	1.1	1.2	1.3	1.4	1.5	1.6	1.7	1.8	1.9	2.0
180	1.6892	0.9236	0.4067	0.3711	0.3440	0.3171	0.2940	0.2751	0.2420	0.2237	0.1033
174	0.3644	0.5372	0.3775	0.3543	0.3203	0.2915	0.2599	0.2666	0.2489	0.3151	0.4113
168	0.2254	0.2703	0.2040	0.1100	0.1001	0.0610	0.0514	0.0681	0.0763	0.4636	0.4075
162	0.2528	0.2493	0.1918	0.1322	0.1806	0.1135	0.0458	0.2035	0.5117	0.4780	0.0706
156	0.3398	0.1964	0.1155	0.1222	0.1864	0.3912	0.5487	0.5490	0.2115	0.0412	0.0409
150	0.2096	0.1220	0.1347	0.1529	0.5766	0.5620	0.2486	0.0909	0.0475	0.0814	0.0613
144	0.2336	0.0772	0.1504	0.5030	0.5117	0.0820	0.0760	0.0504	0.0448	0.0611	0.0735
138	0.1531	0.1412	0.2415	0.3667	0.1695	0.0616	0.0443	0.0467	0.0492	0.0461	0.0563
132	0.1246	0.2727	0.3494	0.3601	0.2303	0.0669	0.0549	0.0562	0.0591	0.0560	0.0532
126	0.4108	0.4198	0.3904	0.3050	0.0981	0.0696	0.0676	0.0601	0.0585	0.0555	0.0527
120	0.4768	0.4445	0.0793	0.0565	0.0795	0.0759	0.0703	0.0615	0.0580	0.0550	0.0522
114	0.4859	0.2142	0.0689	0.0708	0.0606	0.0627	0.0618	0.0581	0.0549	0.0520	0.0494
108	0.4601	0.1895	0.0715	0.0737	0.0635	0.0598	0.0584	0.0549	0.0519	0.0492	0.0467
102	0.4503	0.1763	0.0738	0.0709	0.0647	0.0568	0.0544	0.0523	0.0494	0.0468	0.0425
96	0.4383	0.1545	0.0731	0.0660	0.0659	0.0592	0.0547	0.0514	0.0485	0.0463	0.0442
90	0.4263	0.1455	0.0643	0.0549	0.0696	0.0607	0.0530	0.0487	0.0460	0.0436	0.0434
84	0.4213	0.1386	0.0738	0.0736	0.0735	0.0558	0.0495	0.0466	0.0440	0.0417	0.0397
78	0.4151	0.1311	0.0780	0.0646	0.0537	0.0626	0.0543	0.0499	0.0472	0.0457	0.0434
72	0.4110	0.1494	0.0463	0.0505	0.0716	0.0780	0.0574	0.0538	0.0498	0.0474	0.0449
66	0.4140	0.1696	0.0478	0.0640	0.0854	0.0800	0.0572	0.0549	0.0516	0.0495	0.0455
60	0.4057	0.1508	0.0714	0.0860	0.0933	0.0821	0.0572	0.0572	0.0566	0.0521	0.0478
54	0.4133	0.1584	0.0923	0.0623	0.1228	0.1034	0.0667	0.0630	0.0588	0.0550	0.0539
48	0.4102	0.1847	0.0718	0.1559	0.1552	0.0741	0.0691	0.0643	0.0624	0.0589	0.0532
42	0.3948	0.1865	0.1644	0.1479	0.0459	0.0726	0.0718	0.0675	0.0632	0.0555	0.0524
36	0.3873	0.2044	0.0987	0.0331	0.1167	0.1056	0.0708	0.0713	0.0630	0.0610	0.0627
30	0.3874	0.2118	0.0673	0.1379	0.1311	0.0824	0.0799	0.0737	0.0682	0.0686	0.0660
24	0.3999	0.1647	0.1019	0.1755	0.1242	0.1229	0.0775	0.0683	0.0689	0.0646	0.0663
18	0.4872	0.2535	0.2491	0.1986	0.1343	0.0795	0.0779	0.0842	0.0783	0.0759	0.0744
12	0.5427	0.3352	0.1959	0.0989	0.0984	0.0912	0.0891	0.0821	0.0713	0.0677	0.0607
6	0.5781	0.3140	0.1182	0.1110	0.1049	0.0979	0.0885	0.0725	0.0699	0.0666	0.0630
0	0.5990	0.4665	0.3279	0.3119	0.2896	0.2703	0.2534	0.2385	0.2254	0.2136	0.2027

WHEN TIME =0.000SEC

TABLE 5.9

TEMPERATURE DISTRIBUTION AROUND THE DROPLET

	DIMENSIONLESS RADIUS									
ANGLE	1.0	1.4	1.8	2.2	2.6	3.0	3.4	3.8	4.2	4.6	5.0
180	0.0000	1.0000	1.0000	1.0000	1.0000	1.0000	1.0000	1.0000	1.0000	1.0000	1.0000
174	0.0000	1.0000	1.0000	1.0000	1.0000	1.0000	1.0000	1.0000	1.0000	1.0000	1.0000
168	0.0000	1.0000	1.0000	1.0000	1.0000	1.0000	1.0000	1.0000	1.0000	1.0000	1.0000
162	0.0000	1.0000	1.0000	1.0000	1.0000	1.0000	1.0000	1.0000	1.0000	1.0000	1.0000
156	0.0000	1.0000	1.0000	1.0000	1.0000	1.0000	1.0000	1.0000	1.0000	1.0000	1.0000
150	0.0000	1.0000	1.0000	1.0000	1.0000	1.0000	1.0000	1.0000	1.0000	1.0000	1.0000
144	0.0000	1.0000	1.0000	1.0000	1.0000	1.0000	1.0000	1.0000	1.0000	1.0000	1.0000
138	0.0000	1.0000	1.0000	1.0000	1.0000	1.0000	1.0000	1.0000	1.0000	1.0000	1.0000
132	0.0000	1.0000	1.0000	1.0000	1.0000	1.0000	1.0000	1.0000	1.0000	1.0000	1.0000
126	0.0000	1.0000	1.0000	1.0000	1.0000	1.0000	1.0000	1.0000	1.0000	1.0000	1.0000
120	0.0000	1.0000	1.0000	1.0000	1.0000	1.0000	1.0000	1.0000	1.0000	1.0000	1.0000
114	0.0000	1.0000	1.0000	1.0000	1.0000	1.0000	1.0000	1.0000	1.0000	1.0000	1.0000
108	0.0000	1.0000	1.0000	1.0000	1.0000	1.0000	1.0000	1.0000	1.0000	1.0000	1.0000
102	0.0000	1.0000	1.0000	1.0000	1.0000	1.0000	1.0000	1.0000	1.0000	1.0000	1.0000
96	0.0000	1.0000	1.0000	1.0000	1.0000	1.0000	1.0000	1.0000	1.0000	1.0000	1.0000
90	0.0000	1.0000	1.0000	1.0000	1.0000	1.0000	1.0000	1.0000	1.0000	1.0000	1.0000
84	0.0000	1.0000	1.0000	1.0000	1.0000	1.0000	1.0000	1.0000	1.0000	1.0000	1.0000
78	0.0000	1.0000	1.0000	1.0000	1.0000	1.0000	1.0000	1.0000	1.0000	1.0000	1.0000
72	0.0000	1.0000	1.0000	1.0000	1.0000	1.0000	1.0000	1.0000	1.0000	1.0000	1.0000
66	0.0000	1.0000	1.0000	1.0000	1.0000	1.0000	1.0000	1.0000	1.0000	1.0000	1.0000
60	0.0000	1.0000	1.0000	1.0000	1.0000	1.0000	1.0000	1.0000	1.0000	1.0000	1.0000
54	0.0000	1.0000	1.0000	1.0000	1.0000	1.0000	1.0000	1.0000	1.0000	1.0000	1.0000
48	0.0000	1.0000	1.0000	1.0000	1.0000	1.0000	1.0000	1.0000	1.0000	1.0000	1.0000
42	0.0000	1.0000	1.0000	1.0000	1.0000	1.0000	1.0000	1.0000	1.0000	1.0000	1.0000
36	0.0000	1.0000	1.0000	1.0000	1.0000	1.0000	1.0000	1.0000	1.0000	1.0000	1.0000
30	0.0000	1.0000	1.0000	1.0000	1.0000	1.0000	1.0000	1.0000	1.0000	1.0000	1.0000
24	0.0000	1.0000	1.0000	1.0000	1.0000	1.0000	1.0000	1.0000	1.0000	1.0000	1.0000
18	0.0000	1.0000	1.0000	1.0000	1.0000	1.0000	1.0000	1.0000	1.0000	1.0000	1.0000
12	0.0000	1.0000	1.0000	1.0000	1.0000	1.0000	1.0000	1.0000	1.0000	1.0000	1.0000
6	0.0000	1.0000	1.0000	1.0000	1.0000	1.0000	1.0000	1.0000	1.0000	1.0000	1.0000
0	0.0000	1.0000	1.0000	1.0000	1.0000	1.0000	1.0000	1.0000	1.0000	1.0000	1.0000

WHEN TIME =0.71058762ISEC

TABLE 5.10

TEMPERATURE DISTRIBUTION AROUND THE DROPLET

	DIMENSIONLESS RADIUS										
ANGLE	1.0	1.4	1.8	2.2	2.6	3.0	3.4	3.8	4.2	4.6	5.0
180	0.0936	0.6155	0.9529	0.9989	1.0000	1.0000	1.0000	1.0000	1.0000	1.0000	1.0000
174	0.0934	0.6665	0.9673	0.9995	1.0000	1.0000	1.0000	1.0000	1.0000	1.0000	1.0000
168	0.0937	0.6800	0.9703	0.9996	1.0000	1.0000	1.0000	1.0000	1.0000	1.0000	1.0000
162	0.0940	0.6879	0.9725	0.9997	1.0000	1.0000	1.0000	1.0000	1.0000	1.0000	1.0000
156	0.0944	0.6975	0.9765	0.9997	1.0000	1.0000	1.0000	1.0000	1.0000	1.0000	1.0000
150	0.0945	0.7127	0.9797	0.9998	1.0000	1.0000	1.0000	1.0000	1.0000	1.0000	1.0000
144	0.0948	0.7309	0.9813	0.9998	1.0000	1.0000	1.0000	1.0000	1.0000	1.0000	1.0000
138	0.0951	0.7414	0.9822	0.9998	1.0000	1.0000	1.0000	1.0000	1.0000	1.0000	1.0000
132	0.0956	0.7476	0.9825	0.9998	1.0000	1.0000	1.0000	1.0000	1.0000	1.0000	1.0000
126	0.0969	0.7478	0.9824	0.9998	1.0000	1.0000	1.0000	1.0000	1.0000	1.0000	1.0000
120	0.0974	0.7460	0.9820	0.9998	1.0000	1.0000	1.0000	1.0000	1.0000	1.0000	1.0000
114	0.0970	0.7431	0.9814	0.9998	1.0000	1.0000	1.0000	1.0000	1.0000	1.0000	1.0000
108	0.0970	0.7397	0.9808	0.9997	1.0000	1.0000	1.0000	1.0000	1.0000	1.0000	1.0000
102	0.0970	0.7355	0.9801	0.9997	1.0000	1.0000	1.0000	1.0000	1.0000	1.0000	1.0000
96	0.0969	0.7310	0.9794	0.9997	1.0000	1.0000	1.0000	1.0000	1.0000	1.0000	1.0000
90	0.0968	0.7263	0.9786	0.9997	1.0000	1.0000	1.0000	1.0000	1.0000	1.0000	1.0000
84	0.0967	0.7218	0.9779	0.9997	1.0000	1.0000	1.0000	1.0000	1.0000	1.0000	1.0000
78	0.0966	0.7174	0.9771	0.9997	1.0000	1.0000	1.0000	1.0000	1.0000	1.0000	1.0000
72	0.0964	0.7140	0.9764	0.9996	1.0000	1.0000	1.0000	1.0000	1.0000	1.0000	1.0000
66	0.0963	0.7104	0.9757	0.9996	1.0000	1.0000	1.0000	1.0000	1.0000	1.0000	1.0000
60	0.0961	0.7071	0.9750	0.9996	1.0000	1.0000	1.0000	1.0000	1.0000	1.0000	1.0000
54	0.0959	0.7034	0.9742	0.9996	1.0000	1.0000	1.0000	1.0000	1.0000	1.0000	1.0000
48	0.0956	0.6983	0.9734	0.9996	1.0000	1.0000	1.0000	1.0000	1.0000	1.0000	1.0000
42	0.0953	0.6945	0.9727	0.9996	1.0000	1.0000	1.0000	1.0000	1.0000	1.0000	1.0000
36	0.0950	0.6926	0.9722	0.9995	1.0000	1.0000	1.0000	1.0000	1.0000	1.0000	1.0000
30	0.0947	0.6895	0.9716	0.9995	1.0000	1.0000	1.0000	1.0000	1.0000	1.0000	1.0000
24	0.0944	0.6871	0.9711	0.9995	1.0000	1.0000	1.0000	1.0000	1.0000	1.0000	1.0000
18	0.0941	0.6826	0.9705	0.9995	1.0000	1.0000	1.0000	1.0000	1.0000	1.0000	1.0000
12	0.0938	0.6789	0.9700	0.9995	1.0000	1.0000	1.0000	1.0000	1.0000	1.0000	1.0000
6	0.0934	0.6761	0.9696	0.9995	1.0000	1.0000	1.0000	1.0000	1.0000	1.0000	1.0000
0	0.0930	0.6738	0.9693	0.9995	1.0000	1.0000	1.0000	1.0000	1.0000	1.0000	1.0000

TABLE 5.11

DENSITY DISTRIBUTION AROUND THE DROPLET

ANGLE	DIMENSIONLESS RADIUS										
	1.0	1.4	1.8	2.2	2.6	3.0	3.4	3.8	4.2	4.6	5.0
180	0.0522	0.6042	0.9520	0.9989	1.0000	1.0000	1.0000	1.0000	1.0000	1.0000	1.0000
174	0.0522	0.6569	0.9667	0.9995	1.0000	1.0000	1.0000	1.0000	1.0000	1.0000	1.0000
168	0.0522	0.6709	0.9698	0.9996	1.0000	1.0000	1.0000	1.0000	1.0000	1.0000	1.0000
162	0.0522	0.6791	0.9720	0.9997	1.0000	1.0000	1.0000	1.0000	1.0000	1.0000	1.0000
156	0.0522	0.6888	0.9761	0.9997	1.0000	1.0000	1.0000	1.0000	1.0000	1.0000	1.0000
150	0.0522	0.7045	0.9793	0.9997	1.0000	1.0000	1.0000	1.0000	1.0000	1.0000	1.0000
144	0.0522	0.7233	0.9809	0.9998	1.0000	1.0000	1.0000	1.0000	1.0000	1.0000	1.0000
138	0.0522	0.7341	0.9819	0.9998	1.0000	1.0000	1.0000	1.0000	1.0000	1.0000	1.0000
132	0.0522	0.7404	0.9822	0.9998	1.0000	1.0000	1.0000	1.0000	1.0000	1.0000	1.0000
126	0.0522	0.7407	0.9821	0.9998	1.0000	1.0000	1.0000	1.0000	1.0000	1.0000	1.0000
120	0.0522	0.7388	0.9817	0.9998	1.0000	1.0000	1.0000	1.0000	1.0000	1.0000	1.0000
114	0.0522	0.7359	0.9811	0.9998	1.0000	1.0000	1.0000	1.0000	1.0000	1.0000	1.0000
108	0.0522	0.7324	0.9805	0.9997	1.0000	1.0000	1.0000	1.0000	1.0000	1.0000	1.0000
102	0.0522	0.7280	0.9798	0.9997	1.0000	1.0000	1.0000	1.0000	1.0000	1.0000	1.0000
96	0.0522	0.7233	0.9790	0.9997	1.0000	1.0000	1.0000	1.0000	1.0000	1.0000	1.0000
90	0.0522	0.7185	0.9782	0.9997	1.0000	1.0000	1.0000	1.0000	1.0000	1.0000	1.0000
84	0.0522	0.7139	0.9775	0.9997	1.0000	1.0000	1.0000	1.0000	1.0000	1.0000	1.0000
78	0.0522	0.7094	0.9767	0.9997	1.0000	1.0000	1.0000	1.0000	1.0000	1.0000	1.0000
72	0.0522	0.7058	0.9760	0.9996	1.0000	1.0000	1.0000	1.0000	1.0000	1.0000	1.0000
66	0.0522	0.7022	0.9752	0.9996	1.0000	1.0000	1.0000	1.0000	1.0000	1.0000	1.0000
60	0.0522	0.6988	0.9745	0.9996	1.0000	1.0000	1.0000	1.0000	1.0000	1.0000	1.0000
54	0.0522	0.6950	0.9738	0.9996	1.0000	1.0000	1.0000	1.0000	1.0000	1.0000	1.0000
48	0.0522	0.6898	0.9730	0.9996	1.0000	1.0000	1.0000	1.0000	1.0000	1.0000	1.0000
42	0.0522	0.6858	0.9723	0.9996	1.0000	1.0000	1.0000	1.0000	1.0000	1.0000	1.0000
36	0.0522	0.6839	0.9717	0.9995	1.0000	1.0000	1.0000	1.0000	1.0000	1.0000	1.0000
30	0.0522	0.6806	0.9711	0.9995	1.0000	1.0000	1.0000	1.0000	1.0000	1.0000	1.0000
24	0.0522	0.6782	0.9706	0.9995	1.0000	1.0000	1.0000	1.0000	1.0000	1.0000	1.0000
18	0.0522	0.6735	0.9700	0.9995	1.0000	1.0000	1.0000	1.0000	1.0000	1.0000	1.0000
12	0.0522	0.6698	0.9694	0.9995	1.0000	1.0000	1.0000	1.0000	1.0000	1.0000	1.0000
6	0.0522	0.6669	0.9690	0.9995	1.0000	1.0000	1.0000	1.0000	1.0000	1.0000	1.0000
0	0.0522	0.6645	0.9687	0.9995	1.0000	1.0000	1.0000	1.0000	1.0000	1.0000	1.0000

WHEN TIME =2.1317405705EC

TABLE 5.12

TEMPERATURE DISTRIBUTION AROUND THE DROPLET

	DIMENSIONLESS RADIUS										
ANGLE	1.0	1.4	1.8	2.2	2.6	3.0	3.4	3.8	4.2	4.6	5.0
180	0.1515	0.3457	0.6389	0.8757	0.9836	0.9987	0.9999	1.0000	1.0000	1.0000	1.0000
174	0.1515	0.3850	0.6984	0.9197	0.9890	0.9991	0.9999	1.0000	1.0000	1.0000	1.0000
168	0.1516	0.4011	0.7217	0.9326	0.9910	0.9993	1.0000	1.0000	1.0000	1.0000	1.0000
162	0.1517	0.4156	0.7449	0.9416	0.9922	0.9994	1.0000	1.0000	1.0000	1.0000	1.0000
156	0.1519	0.4333	0.7727	0.9484	0.9931	0.9995	1.0000	1.0000	1.0000	1.0000	1.0000
150	0.1520	0.4561	0.7918	0.9529	0.9937	0.9995	1.0000	1.0000	1.0000	1.0000	1.0000
144	0.1521	0.4781	0.8030	0.9555	0.9940	0.9995	1.0000	1.0000	1.0000	1.0000	1.0000
138	0.1523	0.4907	0.8091	0.9566	0.9941	0.9995	1.0000	1.0000	1.0000	1.0000	1.0000
132	0.1525	0.4973	0.8109	0.9566	0.9941	0.9995	1.0000	1.0000	1.0000	1.0000	1.0000
126	0.1531	0.4974	0.8094	0.9557	0.9939	0.9995	1.0000	1.0000	1.0000	1.0000	1.0000
120	0.1533	0.4942	0.8057	0.9542	0.9935	0.9995	1.0000	1.0000	1.0000	1.0000	1.0000
114	0.1531	0.4891	0.8006	0.9521	0.9931	0.9994	1.0000	1.0000	1.0000	1.0000	1.0000
108	0.1531	0.4829	0.7947	0.9497	0.9926	0.9994	1.0000	1.0000	1.0000	1.0000	1.0000
102	0.1531	0.4758	0.7881	0.9471	0.9921	0.9993	1.0000	1.0000	1.0000	1.0000	1.0000
96	0.1530	0.4683	0.7813	0.9444	0.9915	0.9992	0.9999	1.0000	1.0000	1.0000	1.0000
90	0.1529	0.4607	0.7742	0.9414	0.9908	0.9992	0.9999	1.0000	1.0000	1.0000	1.0000
84	0.1529	0.4534	0.7674	0.9385	0.9902	0.9991	0.9999	1.0000	1.0000	1.0000	1.0000
78	0.1528	0.4463	0.7605	0.9355	0.9895	0.9990	0.9999	1.0000	1.0000	1.0000	1.0000
72	0.1527	0.4399	0.7537	0.9325	0.9889	0.9989	0.9999	1.0000	1.0000	1.0000	1.0000
66	0.1526	0.4335	0.7470	0.9295	0.9882	0.9988	0.9999	1.0000	1.0000	1.0000	1.0000
60	0.1525	0.4275	0.7404	0.9265	0.9874	0.9987	0.9999	1.0000	1.0000	1.0000	1.0000
54	0.1524	0.4215	0.7339	0.9235	0.9867	0.9986	0.9999	1.0000	1.0000	1.0000	1.0000
48	0.1523	0.4149	0.7278	0.9205	0.9860	0.9985	0.9999	1.0000	1.0000	1.0000	1.0000
42	0.1522	0.4095	0.7222	0.9178	0.9853	0.9984	0.9999	1.0000	1.0000	1.0000	1.0000
36	0.1521	0.4055	0.7171	0.9153	0.9847	0.9984	0.9999	1.0000	1.0000	1.0000	1.0000
30	0.1520	0.4010	0.7125	0.9130	0.9841	0.9983	0.9999	1.0000	1.0000	1.0000	1.0000
24	0.1518	0.3976	0.7084	0.9110	0.9836	0.9982	0.9999	1.0000	1.0000	1.0000	1.0000
18	0.1517	0.3934	0.7050	0.9093	0.9831	0.9981	0.9999	1.0000	1.0000	1.0000	1.0000
12	0.1516	0.3901	0.7021	0.9080	0.9828	0.9981	0.9999	1.0000	1.0000	1.0000	1.0000
6	0.1515	0.3876	0.7001	0.9071	0.9825	0.9981	0.9999	1.0000	1.0000	1.0000	1.0000
0	0.1513	0.3853	0.6981	0.9062	0.9823	0.9980	0.9999	1.0000	1.0000	1.0000	1.0000

TABLE 5.13

DENSITY DISTRIBUTION AROUND THE DROPLET

ANGLE	DIMENSIONLESS RADIUS										
	1.0	1.4	1.8	2.2	2.6	3.0	3.4	3.8	4.2	4.6	5.0
180	0.0887	0.3065	0.6218	0.8709	0.9831	0.9987	0.9999	1.0000	1.0000	1.0000	1.0000
174	0.0887	0.3488	0.6844	0.9167	0.9887	0.9991	0.9999	1.0000	1.0000	1.0000	1.0000
168	0.0887	0.3660	0.7089	0.9302	0.9907	0.9993	1.0000	1.0000	1.0000	1.0000	1.0000
162	0.0887	0.3815	0.7332	0.9395	0.9920	0.9994	1.0000	1.0000	1.0000	1.0000	1.0000
156	0.0887	0.4002	0.7623	0.9465	0.9929	0.9994	1.0000	1.0000	1.0000	1.0000	1.0000
150	0.0887	0.4244	0.7824	0.9512	0.9935	0.9995	1.0000	1.0000	1.0000	1.0000	1.0000
144	0.0887	0.4479	0.7941	0.9539	0.9939	0.9995	1.0000	1.0000	1.0000	1.0000	1.0000
138	0.0887	0.4613	0.8005	0.9551	0.9940	0.9995	1.0000	1.0000	1.0000	1.0000	1.0000
132	0.0887	0.4684	0.8024	0.9551	0.9939	0.9995	1.0000	1.0000	1.0000	1.0000	1.0000
126	0.0887	0.4685	0.8009	0.9542	0.9937	0.9995	1.0000	1.0000	1.0000	1.0000	1.0000
120	0.0887	0.4651	0.7971	0.9526	0.9934	0.9994	1.0000	1.0000	1.0000	1.0000	1.0000
114	0.0887	0.4597	0.7917	0.9504	0.9929	0.9994	1.0000	1.0000	1.0000	1.0000	1.0000
108	0.0887	0.4532	0.7855	0.9480	0.9924	0.9993	1.0000	1.0000	1.0000	1.0000	1.0000
102	0.0887	0.4456	0.7786	0.9452	0.9918	0.9993	1.0000	1.0000	1.0000	1.0000	1.0000
96	0.0887	0.4377	0.7715	0.9424	0.9912	0.9992	0.9999	1.0000	1.0000	1.0000	1.0000
90	0.0887	0.4296	0.7641	0.9393	0.9906	0.9991	0.9999	1.0000	1.0000	1.0000	1.0000
84	0.0887	0.4219	0.7569	0.9363	0.9899	0.9991	0.9999	1.0000	1.0000	1.0000	1.0000
78	0.0887	0.4143	0.7498	0.9332	0.9892	0.9990	0.9999	1.0000	1.0000	1.0000	1.0000
72	0.0887	0.4075	0.7426	0.9301	0.9885	0.9989	0.9999	1.0000	1.0000	1.0000	1.0000
66	0.0887	0.4008	0.7356	0.9269	0.9878	0.9988	0.9999	1.0000	1.0000	1.0000	1.0000
60	0.0887	0.3944	0.7287	0.9239	0.9871	0.9987	0.9999	1.0000	1.0000	1.0000	1.0000
54	0.0887	0.3881	0.7219	0.9207	0.9863	0.9986	0.9999	1.0000	1.0000	1.0000	1.0000
48	0.0887	0.3810	0.7155	0.9176	0.9856	0.9985	0.9999	1.0000	1.0000	1.0000	1.0000
42	0.0887	0.3752	0.7096	0.9149	0.9849	0.9984	0.9999	1.0000	1.0000	1.0000	1.0000
36	0.0887	0.3710	0.7043	0.9123	0.9842	0.9983	0.9999	1.0000	1.0000	1.0000	1.0000
30	0.0887	0.3663	0.6995	0.9098	0.9836	0.9982	0.9999	1.0000	1.0000	1.0000	1.0000
24	0.0887	0.3626	0.6952	0.9078	0.9831	0.9982	0.9999	1.0000	1.0000	1.0000	1.0000
18	0.0887	0.3581	0.6917	0.9061	0.9826	0.9981	0.9999	1.0000	1.0000	1.0000	1.0000
12	0.0887	0.3546	0.6886	0.9047	0.9823	0.9980	0.9999	1.0000	1.0000	1.0000	1.0000
6	0.0887	0.3519	0.6865	0.9037	0.9820	0.9980	0.9999	1.0000	1.0000	1.0000	1.0000
0	0.0887	0.3494	0.6843	0.9028	0.9818	0.9980	0.9999	1.0000	1.0000	1.0000	1.0000

WHEN TIME =4.2634668402SEC

TABLE 5.14

TEMPERATURE DISTRIBUTION AROUND THE DROPLET

	DIMENSIONLESS RADIUS										
ANGLE	1.0	1.4	1.8	2.2	2.6	3.0	3.4	3.8	4.2	4.6	5.0
180	0.1921	0.2867	0.4628	0.6927	0.8996	0.9736	0.9945	0.9991	0.9999	1.0000	1.0000
174	0.1921	0.3114	0.5196	0.7647	0.9190	0.9784	0.9956	0.9993	0.9999	1.0000	1.0000
168	0.1921	0.3233	0.5462	0.7897	0.9278	0.9809	0.9961	0.9994	0.9999	1.0000	1.0000
162	0.1922	0.3354	0.5735	0.8080	0.9342	0.9826	0.9964	0.9994	0.9999	1.0000	1.0000
156	0.1923	0.3497	0.6039	0.8218	0.9387	0.9838	0.9967	0.9995	0.9999	1.0000	1.0000
150	0.1924	0.3672	0.6245	0.8309	0.9416	0.9845	0.9968	0.9995	0.9999	1.0000	1.0000
144	0.1925	0.3832	0.6363	0.8358	0.9429	0.9847	0.9968	0.9995	0.9999	1.0000	1.0000
138	0.1925	0.3920	0.6421	0.8372	0.9429	0.9846	0.9968	0.9995	0.9999	1.0000	1.0000
132	0.1927	0.3959	0.6426	0.8358	0.9417	0.9841	0.9966	0.9994	0.9999	1.0000	1.0000
126	0.1930	0.3949	0.6389	0.8320	0.9395	0.9832	0.9964	0.9994	0.9999	1.0000	1.0000
120	0.1931	0.3911	0.6323	0.8263	0.9364	0.9820	0.9961	0.9993	0.9999	1.0000	1.0000
114	0.1930	0.3855	0.6237	0.8192	0.9325	0.9805	0.9957	0.9992	0.9999	1.0000	1.0000
108	0.1930	0.3791	0.6139	0.8112	0.9281	0.9788	0.9952	0.9991	0.9999	1.0000	1.0000
102	0.1930	0.3719	0.6033	0.8024	0.9233	0.9769	0.9946	0.9990	0.9998	1.0000	1.0000
96	0.1929	0.3644	0.5924	0.7933	0.9182	0.9749	0.9940	0.9989	0.9998	1.0000	1.0000
90	0.1928	0.3570	0.5812	0.7838	0.9127	0.9727	0.9934	0.9988	0.9998	1.0000	1.0000
84	0.1928	0.3498	0.5704	0.7745	0.9073	0.9704	0.9927	0.9986	0.9998	1.0000	1.0000
78	0.1927	0.3429	0.5597	0.7651	0.9017	0.9680	0.9920	0.9984	0.9997	1.0000	1.0000
72	0.1927	0.3366	0.5493	0.7556	0.8960	0.9656	0.9912	0.9983	0.9997	1.0000	1.0000
66	0.1926	0.3306	0.5392	0.7464	0.8904	0.9631	0.9904	0.9981	0.9997	0.9999	1.0000
60	0.1926	0.3249	0.5296	0.7375	0.8847	0.9606	0.9896	0.9979	0.9996	0.9999	1.0000
54	0.1925	0.3195	0.5205	0.7288	0.8792	0.9581	0.9887	0.9977	0.9996	0.9999	1.0000
48	0.1925	0.3141	0.5120	0.7204	0.8736	0.9555	0.9878	0.9974	0.9996	0.9999	1.0000
42	0.1924	0.3095	0.5043	0.7129	0.8686	0.9531	0.9870	0.9972	0.9995	0.9999	1.0000
36	0.1923	0.3060	0.4976	0.7060	0.8640	0.9508	0.9862	0.9970	0.9995	0.9999	1.0000
30	0.1923	0.3024	0.4916	0.6999	0.8598	0.9488	0.9855	0.9968	0.9994	0.9999	1.0000
24	0.1922	0.2997	0.4865	0.6948	0.8563	0.9471	0.9849	0.9967	0.9994	0.9999	1.0000
18	0.1922	0.2968	0.4825	0.6907	0.8534	0.9457	0.9844	0.9965	0.9994	0.9999	1.0000
12	0.1921	0.2947	0.4792	0.6876	0.8513	0.9446	0.9840	0.9964	0.9994	0.9999	1.0000
6	0.1921	0.2931	0.4770	0.6854	0.8497	0.9438	0.9837	0.9963	0.9994	0.9999	1.0000
0	0.1920	0.2917	0.4748	0.6833	0.8483	0.9431	0.9834	0.9963	0.9993	0.9999	1.0000

TABLE 5.15

DENSITY DISTRIBUTION AROUND THE DROPLET

	DIMENSIONLESS RADIUS										
ANGLE	1.0	1.4	1.8	2.2	2.6	3.0	3.4	3.8	4.2	4.6	5.0
180	0.1161	0.2268	0.4234	0.6729	0.8941	0.9723	0.9943	0.9991	0.9999	1.0000	1.0000
174	0.1161	0.2543	0.4851	0.7502	0.9147	0.9775	0.9954	0.9993	0.9999	1.0000	1.0000
168	0.1161	0.2675	0.5138	0.7768	0.9241	0.9800	0.9959	0.9993	0.9999	1.0000	1.0000
162	0.1161	0.2807	0.5433	0.7964	0.9308	0.9818	0.9963	0.9994	0.9999	1.0000	1.0000
156	0.1161	0.2964	0.5762	0.8112	0.9356	0.9830	0.9966	0.9994	0.9999	1.0000	1.0000
150	0.1161	0.3156	0.5985	0.8209	0.9386	0.9838	0.9967	0.9995	0.9999	1.0000	1.0000
144	0.1161	0.3332	0.6113	0.8262	0.9401	0.9841	0.9967	0.9995	0.9999	1.0000	1.0000
138	0.1161	0.3430	0.6176	0.8277	0.9400	0.9839	0.9967	0.9994	0.9999	1.0000	1.0000
132	0.1161	0.3474	0.6182	0.8262	0.9388	0.9834	0.9965	0.9994	0.9999	1.0000	1.0000
126	0.1161	0.3463	0.6143	0.8222	0.9364	0.9824	0.9963	0.9994	0.9999	1.0000	1.0000
120	0.1161	0.3421	0.6072	0.8162	0.9332	0.9812	0.9959	0.9993	0.9999	1.0000	1.0000
114	0.1161	0.3362	0.5980	0.8086	0.9291	0.9797	0.9955	0.9992	0.9999	1.0000	1.0000
108	0.1161	0.3291	0.5875	0.8001	0.9245	0.9779	0.9950	0.9991	0.9999	1.0000	1.0000
102	0.1161	0.3213	0.5761	0.7909	0.9194	0.9759	0.9944	0.9990	0.9998	1.0000	1.0000
96	0.1161	0.3132	0.5644	0.7812	0.9140	0.9738	0.9938	0.9989	0.9998	1.0000	1.0000
90	0.1161	0.3051	0.5525	0.7711	0.9083	0.9715	0.9931	0.9987	0.9998	1.0000	1.0000
84	0.1161	0.2973	0.5409	0.7613	0.9026	0.9691	0.9924	0.9986	0.9998	1.0000	1.0000
78	0.1161	0.2898	0.5294	0.7512	0.8967	0.9666	0.9917	0.9984	0.9997	1.0000	1.0000
72	0.1161	0.2830	0.5182	0.7412	0.8907	0.9641	0.9909	0.9982	0.9997	1.0000	1.0000
66	0.1161	0.2763	0.5074	0.7314	0.8848	0.9615	0.9900	0.9980	0.9997	0.9999	1.0000
60	0.1161	0.2702	0.4971	0.7219	0.8788	0.9588	0.9892	0.9978	0.9996	0.9999	1.0000
54	0.1161	0.2643	0.4872	0.7127	0.8730	0.9562	0.9883	0.9976	0.9996	0.9999	1.0000
48	0.1161	0.2584	0.4781	0.7037	0.8672	0.9535	0.9874	0.9973	0.9996	0.9999	1.0000
42	0.1161	0.2534	0.4699	0.6958	0.8619	0.9510	0.9865	0.9971	0.9995	0.9999	1.0000
36	0.1161	0.2495	0.4626	0.6885	0.8570	0.9486	0.9857	0.9969	0.9995	0.9999	1.0000
30	0.1161	0.2456	0.4561	0.6820	0.8526	0.9465	0.9849	0.9967	0.9994	0.9999	1.0000
24	0.1161	0.2426	0.4507	0.6765	0.8489	0.9447	0.9843	0.9965	0.9994	0.9999	1.0000
18	0.1161	0.2394	0.4463	0.6722	0.8459	0.9432	0.9837	0.9964	0.9994	0.9999	1.0000
12	0.1161	0.2371	0.4428	0.6689	0.8436	0.9421	0.9833	0.9963	0.9993	0.9999	1.0000
6	0.1161	0.2353	0.4404	0.6666	0.8420	0.9412	0.9830	0.9962	0.9993	0.9999	1.0000
0	0.1161	0.2337	0.4381	0.6643	0.8405	0.9405	0.9828	0.9961	0.9993	0.9999	1.0000

WHEN TIME =6.039905550SEC

TABLE 5.16

TEMPERATURE DISTRIBUTION AROUND THE DROPLET

	DIMENSIONLESS RADIUS									
ANGLE	1.0	1.4	1.8	2.2	2.6	3.0	3.4	3.8	4.2	4.6	5.0
180	0.2125	0.2806	0.4154	0.6185	0.8382	0.9402	0.9813	0.9951	0.9989	0.9998	1.0000
174	0.2124	0.2995	0.4639	0.6885	0.8604	0.9476	0.9836	0.9957	0.9990	0.9998	1.0000
168	0.2125	0.3089	0.4872	0.7132	0.8709	0.9515	0.9848	0.9960	0.9991	0.9998	1.0000
162	0.2125	0.3185	0.5112	0.7314	0.8786	0.9543	0.9857	0.9963	0.9992	0.9998	1.0000
156	0.2126	0.3299	0.5374	0.7449	0.8840	0.9562	0.9863	0.9964	0.9992	0.9998	1.0000
150	0.2126	0.3436	0.5547	0.7534	0.8871	0.9572	0.9865	0.9965	0.9992	0.9998	1.0000
144	0.2127	0.3558	0.5640	0.7572	0.8880	0.9572	0.9864	0.9964	0.9992	0.9998	1.0000
138	0.2128	0.3621	0.5678	0.7572	0.8868	0.9562	0.9859	0.9962	0.9991	0.9998	1.0000
132	0.2129	0.3644	0.5666	0.7538	0.8839	0.9545	0.9852	0.9960	0.9991	0.9998	1.0000
126	0.2131	0.3626	0.5615	0.7477	0.8792	0.9519	0.9841	0.9956	0.9990	0.9998	1.0000
120	0.2132	0.3586	0.5536	0.7394	0.8731	0.9486	0.9827	0.9951	0.9989	0.9998	1.0000
114	0.2131	0.3531	0.5438	0.7292	0.8657	0.9445	0.9809	0.9945	0.9987	0.9997	1.0000
108	0.2131	0.3469	0.5329	0.7180	0.8575	0.9399	0.9789	0.9938	0.9985	0.9997	1.0000
102	0.2131	0.3401	0.5212	0.7060	0.8485	0.9348	0.9766	0.9930	0.9983	0.9996	1.0000
96	0.2130	0.3332	0.5094	0.6936	0.8391	0.9294	0.9742	0.9921	0.9980	0.9996	1.0000
90	0.2130	0.3264	0.4975	0.6809	0.8293	0.9236	0.9715	0.9911	0.9977	0.9995	1.0000
84	0.2129	0.3199	0.4860	0.6685	0.8196	0.9178	0.9687	0.9901	0.9974	0.9994	1.0000
78	0.2129	0.3137	0.4748	0.6561	0.8097	0.9117	0.9658	0.9890	0.9970	0.9993	1.0000
72	0.2128	0.3080	0.4640	0.6439	0.7999	0.9056	0.9628	0.9878	0.9966	0.9992	1.0000
66	0.2128	0.3027	0.4538	0.6322	0.7902	0.8995	0.9597	0.9865	0.9962	0.9991	1.0000
60	0.2127	0.2977	0.4441	0.6210	0.7807	0.8932	0.9565	0.9852	0.9958	0.9990	1.0000
54	0.2127	0.2932	0.4351	0.6103	0.7715	0.8872	0.9533	0.9839	0.9954	0.9989	1.0000
48	0.2127	0.2887	0.4268	0.6001	0.7625	0.8810	0.9501	0.9825	0.9949	0.9988	1.0000
42	0.2126	0.2850	0.4195	0.5911	0.7544	0.8754	0.9470	0.9812	0.9944	0.9986	1.0000
36	0.2126	0.2820	0.4131	0.5829	0.7470	0.8703	0.9442	0.9799	0.9940	0.9985	1.0000
30	0.2126	0.2792	0.4074	0.5758	0.7405	0.8658	0.9417	0.9788	0.9936	0.9984	1.0000
24	0.2125	0.2770	0.4028	0.5699	0.7351	0.8619	0.9395	0.9778	0.9932	0.9983	1.0000
18	0.2125	0.2748	0.3991	0.5652	0.7307	0.8587	0.9377	0.9770	0.9929	0.9982	1.0000
12	0.2125	0.2732	0.3962	0.5617	0.7274	0.8563	0.9363	0.9764	0.9927	0.9981	1.0000
6	0.2124	0.2721	0.3942	0.5593	0.7250	0.8546	0.9353	0.9759	0.9925	0.9981	1.0000
0	0.2124	0.2710	0.3923	0.5569	0.7229	0.8531	0.9345	0.9755	0.9924	0.9981	1.0000

TABLE 5.17

DENSITY DISTRIBUTION AROUND THE DROPLET

	DIMENSIONLESS RADIUS										
ANGLE	1.0	1.4	1.8	2.2	2.6	3.0	3.4	3.8	4.2	4.6	5.0
180	0.1304	0.2114	0.3643	0.5884	0.8270	0.9366	0.9802	0.9948	0.9989	0.9998	1.0000
174	0.1304	0.2328	0.4180	0.6648	0.8510	0.9445	0.9827	0.9955	0.9990	0.9998	1.0000
168	0.1304	0.2434	0.4436	0.6917	0.8624	0.9486	0.9840	0.9958	0.9991	0.9998	1.0000
162	0.1304	0.2542	0.4700	0.7115	0.8707	0.9517	0.9850	0.9961	0.9991	0.9998	1.0000
156	0.1304	0.2669	0.4989	0.7262	0.8765	0.9537	0.9856	0.9962	0.9992	0.9998	1.0000
150	0.1304	0.2822	0.5180	0.7355	0.8799	0.9547	0.9858	0.9963	0.9992	0.9998	1.0000
144	0.1304	0.2959	0.5284	0.7398	0.8809	0.9547	0.9857	0.9962	0.9992	0.9998	1.0000
138	0.1304	0.3030	0.5326	0.7397	0.8796	0.9538	0.9852	0.9961	0.9991	0.9998	1.0000
132	0.1304	0.3057	0.5314	0.7362	0.8765	0.9519	0.9844	0.9958	0.9990	0.9998	1.0000
126	0.1304	0.3038	0.5259	0.7296	0.8715	0.9492	0.9833	0.9954	0.9989	0.9998	1.0000
120	0.1304	0.2994	0.5174	0.7207	0.8650	0.9456	0.9818	0.9949	0.9988	0.9998	1.0000
114	0.1304	0.2934	0.5067	0.7098	0.8571	0.9413	0.9799	0.9943	0.9986	0.9997	1.0000
108	0.1304	0.2865	0.4949	0.6978	0.8484	0.9365	0.9778	0.9936	0.9984	0.9997	1.0000
102	0.1304	0.2791	0.4823	0.6849	0.8389	0.9311	0.9755	0.9927	0.9982	0.9996	1.0000
96	0.1304	0.2715	0.4694	0.6716	0.8289	0.9254	0.9729	0.9918	0.9979	0.9996	1.0000
90	0.1304	0.2640	0.4564	0.6579	0.8184	0.9193	0.9700	0.9907	0.9976	0.9995	1.0000
84	0.1304	0.2568	0.4440	0.6446	0.8080	0.9131	0.9671	0.9896	0.9973	0.9994	1.0000
78	0.1304	0.2499	0.4318	0.6312	0.7975	0.9067	0.9640	0.9884	0.9969	0.9993	1.0000
72	0.1304	0.2437	0.4200	0.6181	0.7870	0.9001	0.9608	0.9872	0.9965	0.9992	1.0000
66	0.1304	0.2378	0.4088	0.6055	0.7767	0.8937	0.9576	0.9859	0.9961	0.9991	1.0000
60	0.1304	0.2323	0.3983	0.5934	0.7665	0.8871	0.9543	0.9845	0.9956	0.9990	1.0000
54	0.1304	0.2272	0.3884	0.5818	0.7567	0.8807	0.9509	0.9831	0.9952	0.9989	1.0000
48	0.1304	0.2222	0.3794	0.5708	0.7471	0.8742	0.9475	0.9817	0.9947	0.9987	1.0000
42	0.1304	0.2181	0.3714	0.5611	0.7384	0.8682	0.9443	0.9803	0.9942	0.9986	1.0000
36	0.1304	0.2148	0.3643	0.5523	0.7305	0.8628	0.9413	0.9790	0.9937	0.9985	1.0000
30	0.1304	0.2116	0.3582	0.5446	0.7236	0.8579	0.9386	0.9778	0.9933	0.9983	1.0000
24	0.1304	0.2092	0.3530	0.5382	0.7178	0.8538	0.9363	0.9768	0.9929	0.9982	1.0000
18	0.1304	0.2067	0.3490	0.5331	0.7130	0.8505	0.9344	0.9759	0.9926	0.9981	1.0000
12	0.1304	0.2049	0.3458	0.5294	0.7095	0.8479	0.9330	0.9753	0.9924	0.9981	1.0000
6	0.1304	0.2036	0.3436	0.5267	0.7070	0.8461	0.9320	0.9748	0.9922	0.9980	1.0000
0	0.1304	0.2024	0.3415	0.5242	0.7047	0.8445	0.9310	0.9744	0.9920	0.9980	1.0000

WHEN TIME =8.526920320SEC

TABLE 5.18

TEMPERATURE DISTRIBUTION AROUND THE DROPLET

	DIMENSIONLESS RADIUS										
ANGLE	1.0	1.4	1.8	2.2	2.6	3.0	3.4	3.8	4.2	4.6	5.0
180	0.2320	0.2827	0.3877	0.5628	0.7768	0.8956	0.9564	0.9839	0.9948	0.9986	1.0000
174	0.2320	0.2971	0.4274	0.6249	0.7976	0.9037	0.9596	0.9851	0.9952	0.9987	1.0000
168	0.2320	0.3043	0.4464	0.6463	0.8075	0.9078	0.9612	0.9857	0.9954	0.9988	1.0000
162	0.2321	0.3116	0.4657	0.6617	0.8144	0.9107	0.9624	0.9861	0.9955	0.9988	1.0000
156	0.2321	0.3202	0.4866	0.6725	0.8187	0.9123	0.9628	0.9862	0.9955	0.9988	1.0000
150	0.2321	0.3303	0.4995	0.6785	0.8204	0.9124	0.9626	0.9860	0.9954	0.9988	1.0000
144	0.2322	0.3391	0.5056	0.6799	0.8194	0.9110	0.9617	0.9856	0.9952	0.9987	1.0000
138	0.2323	0.3431	0.5069	0.6773	0.8158	0.9081	0.9599	0.9847	0.9949	0.9986	1.0000
132	0.2323	0.3439	0.5038	0.6715	0.8099	0.9039	0.9575	0.9835	0.9944	0.9984	1.0000
126	0.2325	0.3415	0.4973	0.6628	0.8019	0.8982	0.9542	0.9820	0.9938	0.9982	1.0000
120	0.2325	0.3373	0.4885	0.6519	0.7920	0.8912	0.9501	0.9800	0.9930	0.9980	1.0000
114	0.2325	0.3320	0.4780	0.6391	0.7806	0.8829	0.9452	0.9776	0.9920	0.9976	1.0000
108	0.2324	0.3263	0.4667	0.6254	0.7681	0.8739	0.9398	0.9748	0.9908	0.9972	1.0000
102	0.2324	0.3202	0.4549	0.6110	0.7548	0.8640	0.9338	0.9717	0.9894	0.9967	1.0000
96	0.2324	0.3141	0.4431	0.5964	0.7410	0.8536	0.9273	0.9683	0.9879	0.9962	1.0000
90	0.2323	0.3081	0.4314	0.5817	0.7269	0.8427	0.9203	0.9646	0.9862	0.9956	1.0000
84	0.2323	0.3025	0.4203	0.5675	0.7131	0.8319	0.9133	0.9607	0.9844	0.9949	1.0000
78	0.2323	0.2972	0.4096	0.5535	0.6993	0.8208	0.9059	0.9566	0.9825	0.9942	1.0000
72	0.2322	0.2925	0.3995	0.5401	0.6858	0.8098	0.8985	0.9523	0.9804	0.9933	1.0000
66	0.2322	0.2880	0.3901	0.5274	0.6728	0.7991	0.8911	0.9480	0.9783	0.9925	1.0000
60	0.2322	0.2840	0.3814	0.5154	0.6602	0.7883	0.8835	0.9435	0.9760	0.9916	1.0000
54	0.2321	0.2804	0.3733	0.5042	0.6483	0.7781	0.8761	0.9390	0.9737	0.9906	1.0000
48	0.2321	0.2769	0.3661	0.4938	0.6368	0.7679	0.8687	0.9344	0.9713	0.9896	1.0000
42	0.2321	0.2740	0.3598	0.4846	0.6266	0.7588	0.8619	0.9302	0.9690	0.9886	1.0000
36	0.2321	0.2717	0.3543	0.4764	0.6175	0.7505	0.8556	0.9262	0.9669	0.9877	1.0000
30	0.2320	0.2696	0.3496	0.4694	0.6096	0.7433	0.8501	0.9226	0.9649	0.9868	1.0000
24	0.2320	0.2680	0.3457	0.4637	0.6030	0.7372	0.8454	0.9196	0.9633	0.9861	1.0000
18	0.2320	0.2665	0.3426	0.4591	0.5977	0.7323	0.8416	0.9171	0.9619	0.9854	1.0000
12	0.2320	0.2654	0.3403	0.4558	0.5938	0.7286	0.8387	0.9152	0.9608	0.9850	1.0000
6	0.2320	0.2646	0.3387	0.4534	0.5910	0.7259	0.8367	0.9138	0.9600	0.9846	1.0000
0	0.2320	0.2638	0.3372	0.4511	0.5884	0.7235	0.8348	0.9126	0.9594	0.9843	1.0000

TABLE 5.19

DENSITY DISTRIBUTION AROUND THE DROPLET

	DIMENSIONLESS RADIUS										
ANGLE	1.0	1.4	1.8	2.2	2.6	3.0	3.4	3.8	4.2	4.6	5.0
180	0.1445	0.2054	0.3261	0.5221	0.7582	0.8878	0.9534	0.9829	0.9945	0.9985	1.0000
174	0.1445	0.2220	0.3708	0.5911	0.7812	0.8966	0.9569	0.9841	0.9949	0.9986	1.0000
168	0.1445	0.2303	0.3920	0.6148	0.7920	0.9011	0.9587	0.9848	0.9951	0.9987	1.0000
162	0.1445	0.2386	0.4137	0.6320	0.7997	0.9043	0.9599	0.9852	0.9953	0.9987	1.0000
156	0.1445	0.2483	0.4372	0.6440	0.8044	0.9060	0.9604	0.9854	0.9953	0.9987	1.0000
150	0.1445	0.2599	0.4518	0.6508	0.8063	0.9061	0.9602	0.9852	0.9952	0.9987	1.0000
144	0.1445	0.2699	0.4588	0.6524	0.8053	0.9047	0.9592	0.9847	0.9950	0.9986	1.0000
138	0.1445	0.2746	0.4603	0.6498	0.8015	0.9016	0.9574	0.9838	0.9946	0.9985	1.0000
132	0.1445	0.2756	0.4571	0.6435	0.7952	0.8971	0.9547	0.9826	0.9941	0.9984	1.0000
126	0.1445	0.2730	0.4500	0.6341	0.7866	0.8910	0.9512	0.9809	0.9935	0.9981	1.0000
120	0.1445	0.2684	0.4404	0.6222	0.7760	0.8835	0.9469	0.9788	0.9926	0.9979	1.0000
114	0.1445	0.2626	0.4288	0.6084	0.7636	0.8747	0.9417	0.9762	0.9915	0.9975	1.0000
108	0.1445	0.2562	0.4164	0.5934	0.7501	0.8650	0.9359	0.9733	0.9903	0.9971	1.0000
102	0.1445	0.2493	0.4034	0.5777	0.7358	0.8544	0.9295	0.9700	0.9889	0.9966	1.0000
96	0.1445	0.2425	0.3904	0.5618	0.7209	0.8432	0.9226	0.9664	0.9873	0.9960	1.0000
90	0.1445	0.2359	0.3775	0.5457	0.7056	0.8316	0.9152	0.9624	0.9855	0.9953	1.0000
84	0.1445	0.2296	0.3652	0.5302	0.6906	0.8199	0.9076	0.9583	0.9836	0.9946	1.0000
78	0.1445	0.2237	0.3534	0.5150	0.6757	0.8081	0.8998	0.9540	0.9815	0.9939	1.0000
72	0.1445	0.2183	0.3422	0.5003	0.6611	0.7962	0.8919	0.9495	0.9793	0.9930	1.0000
66	0.1445	0.2133	0.3318	0.4864	0.6470	0.7847	0.8839	0.9449	0.9771	0.9921	1.0000
60	0.1445	0.2088	0.3221	0.4733	0.6333	0.7731	0.8758	0.9401	0.9747	0.9911	1.0000
54	0.1445	0.2047	0.3132	0.4610	0.6204	0.7621	0.8680	0.9354	0.9722	0.9901	1.0000
48	0.1445	0.2008	0.3051	0.4495	0.6080	0.7512	0.8600	0.9305	0.9697	0.9890	1.0000
42	0.1445	0.1975	0.2981	0.4394	0.5969	0.7413	0.8527	0.9259	0.9673	0.9880	1.0000
36	0.1445	0.1949	0.2919	0.4305	0.5870	0.7324	0.8460	0.9217	0.9650	0.9870	1.0000
30	0.1445	0.1925	0.2867	0.4227	0.5784	0.7246	0.8401	0.9179	0.9630	0.9861	1.0000
24	0.1445	0.1906	0.2824	0.4164	0.5712	0.7180	0.8351	0.9147	0.9612	0.9853	1.0000
18	0.1445	0.1889	0.2789	0.4114	0.5655	0.7127	0.8310	0.9120	0.9597	0.9847	1.0000
12	0.1445	0.1876	0.2763	0.4077	0.5612	0.7087	0.8279	0.9100	0.9586	0.9842	1.0000
6	0.1445	0.1867	0.2745	0.4051	0.5582	0.7059	0.8257	0.9086	0.9578	0.9838	1.0000
0	0.1445	0.1858	0.2728	0.4026	0.5553	0.7033	0.8237	0.9073	0.9571	0.9835	1.0000

CONCLUSION

The aim of the study was to provide a fundamental basis for the numerical simulation of the heat transfer problem involving the condensation of steam onto a spray of water drops, such as in a contact condenser. We worked with single droplet but this method, while having the advantage of being more manageable theoretically, is different from the actual practical condition. On the surface of the droplet, condensation occurs with consequent heat absorption. It is evident from an examination of the temperature-time characteristic that the average droplet temperature increases with increasing time. This is as would be expected. However, the results also shows that it takes much longer to heat up large drops than small drops.

Three models were reviewed for the heat transport process in the droplet; of these, the complete mixing model was used in this study. Values of the average heat and mass transfer coefficients were calculated from the data obtained from the program and the value of the heat transfer coefficient was compared with the theoretical result of Brown (2). It can be concluded from the result of the study that the complete mixing model could describe the cooling behavior of 3 mm water droplet falling freeling in a steam atmosphere. The heat and mass transfer of large spray drops can be influenced by its strong oscillation but was not described in the present study.

Thus, although the thermal and hydrodynamic behavior of the droplets are sufficiently well known and quantifiable, the accurate prediction of the overall performance of cooling systems still remains difficult and somewhat uncertain.

REFERENCES

1. Arnold,H.D., Phil. Mag., 22, 755 (1911).

2. Brown,G.,"Heat Transmission by Condensation of Steam on a Spray of Water Drops," ASME, Proc. Gen. Disc. Heat Transfer, 49-52 (1951).

3. Chao,B.T.,"Transient Heat and Mass Transfer to a Translating Droplet," J. Heat Transfer, Trans. ASME, 91, 273-281 (1969).

4. Dickinson,D.R.,and W.R. Marshall,Jr.,"The Rates of Evaporation of Sprays," A.I.Ch.E. Journal, 14,541-552 (1968).

5. Frossling,N.,"Evaporation,Heat Transfer and Velocity Distribution in Two-Dimensional and Rotationally Symmetrical Boundary Layer Flow," Report NACA TM 1432 (1958).

6. Gal-or,B.,and S. Waslo,"Hydrodynamics of an Ensemble of Drops(or Bubbles) in the Presence or Absence of Surfactants," Chem. Eng. Sci., 23, 1431-1446 (1968).

7. Goldstein,S., Proc. Roy. Soc.(London), 123, 225 (1929).

8. Hadarmard,C., J. Acad. Sci., Paris 152, 1735 (1911).

9. Happel,J.,"Viscous Flow in Multiparticle System: Slow Motion of Fluids Relative to Beds of Spherical Particles," A.I.Ch.E. J., 4, 197-201 (1958).

10. Harpole,G.M.,"Droplet Evaporation in High Temperature Environments," Transactions of the ASME, Vol.103 (1981).

11. Johnstone,H.F.,and G.C. Williams, Ind. Eng. Chem., August,(1939).

12. Konopliv,N.,and Sparrow,E.,"Unsteady Heat Transfer and Temperature for Stokesian Flow About a Sphere," Journal of Heat Transfer, Trans. ASME, Vol.94,266-272(Aug.1974).

13. Kronig,R.,and J.C. Brink,"On the Theory of Extraction from Falling Droplets," Appl. Sci. Res.,A2,142 (1950).

14 Kulic,E.,Rhodes,E.,and Sullivan,G.,"Heat Transfer Rate Predictions in Condensation on Droplets from Air/Steam Mixtures," The Canadian Journal of Chemical Engineering, 53, 252-258 (1975).

15. Lamb,H., HYDRODYNAMICS Sixth Edition, Cambridge University Press, pp 450-475, 639-641 (1932).

16. Laws,J.O.,"Measurement of the Fall Velocity of Water-Drops and Raindrops," Trans. Amer. Geophys. Union, 22, Part III, 709-721 (1941).

17. Lapple,C.E., FLUID AND PARTICLE MECHANICS, University of Delaware, p 284 (1951).

18. Lee,K.,and D.J. Ryley,"The Evaporation of Water Droplets in Superheated Steam," J. Heat Transfer, Trans. ASME,90, 445-451 (1968).

19. Lenard,P., Ann. Physik, 65, 629 (1921).

20. Levich,V.G., PHYSICOCHEMICAL HYDRODYNAMICS, Prentice Hall , Inc. (1962).

21. Manno,V.,"Analytical Modeling of Hydrogen Transport in Reactor Containment," Sc.D Thesis, M.I.T. August 1983.

22. Oseen,C.W., Arkiv. Mat. Astron. Fysik, 9, 1 (1913).

23. Powell,R.E., Industr. Engng. Chem., 33, 430 (1941).

24. Ranz,W.E. and W.R. Marshall,Jr.,"Evaporation from Drops," Chem. Eng. Progr. 48, 141-146, 173-180 (1952).

25. Richtmyer,R.D., DIFFERENCE METHODS FOR INITIAL-VALUE PROBLEMS, Interscience Publ., New York, p98 (1957).

26. Rimon,Y.and S.I. Cheng,"Numerical Solution of a Uniform Flow over a Sphere at Intermediate Reynolds Number," Phy. Fluids, Vol. 12, No. 5 (May 1969).

27. Roache,P.J., COMPUTATIONAL FLUID DYNAMICS, Chap. 3, Hermosa, Albuquerque (1972).

28. Rouse,H., FLUID MECHANICS FOR HYDRAULIC ENGINEERS, New York, Mc-Graw Hill Book Co. (1938).

29. Rowe,P.N., Claxton,K.T.and J.B. Lewis,"Heat and Mass Transfer from a Single Sphere in an Extensive Flowing Fluid," Trans. Instn. Chem. Engrs., 43, 14-31 (1965).

30. Ruckenstein,E.,"Mass Transfer Between a Single Drop and a Continuous Phase," Int. J. Heat Mass Transfer, 10, 1785-1792 (1967).

31. Saito,S., Science Reports, Tohoku Imp. Univ.,2,179 (1913).

32. Schlichting,H., BOUNDARY LAYER THEORY, Sixth Edition, McGraw-Hill, p 403 (1966).

33. Smagorinsky,J.,"General Circulation Experiments with the Primitive Equations," Monthly Weather Review 91,99 (1963).

34. Smith,G.D., NUMERICAL SOLUTION OF PARTIAL DIFFERENTIAL EQUATIONS, Chaps.2 and 5, Oxford Univ. Press,London(1965).

35. Spilhaus,A.F., J. Met., 5, 108 (1948).

36. Squires,L. and W. Squires,Jr., Trans. Am. Inst. Chem. Engrs., 33, 1-12 (1937).

37. Wadell,H., Physics, 5, 281-291 (1934).

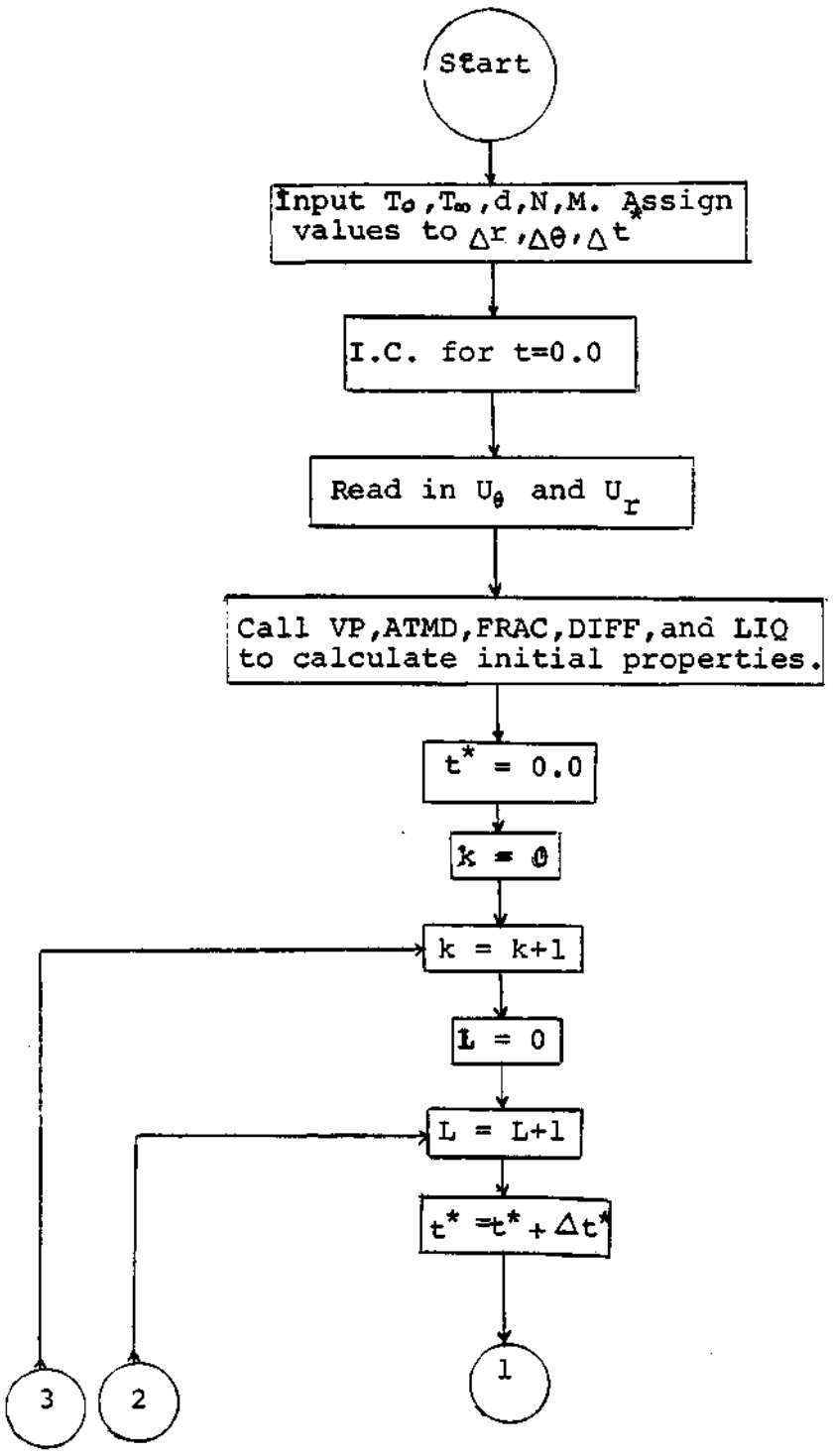
38. Winnikow,S.and B.T. Chao,"Droplet Motion in Purified Systems," Physics of Fluids, 9, 50 (1966).

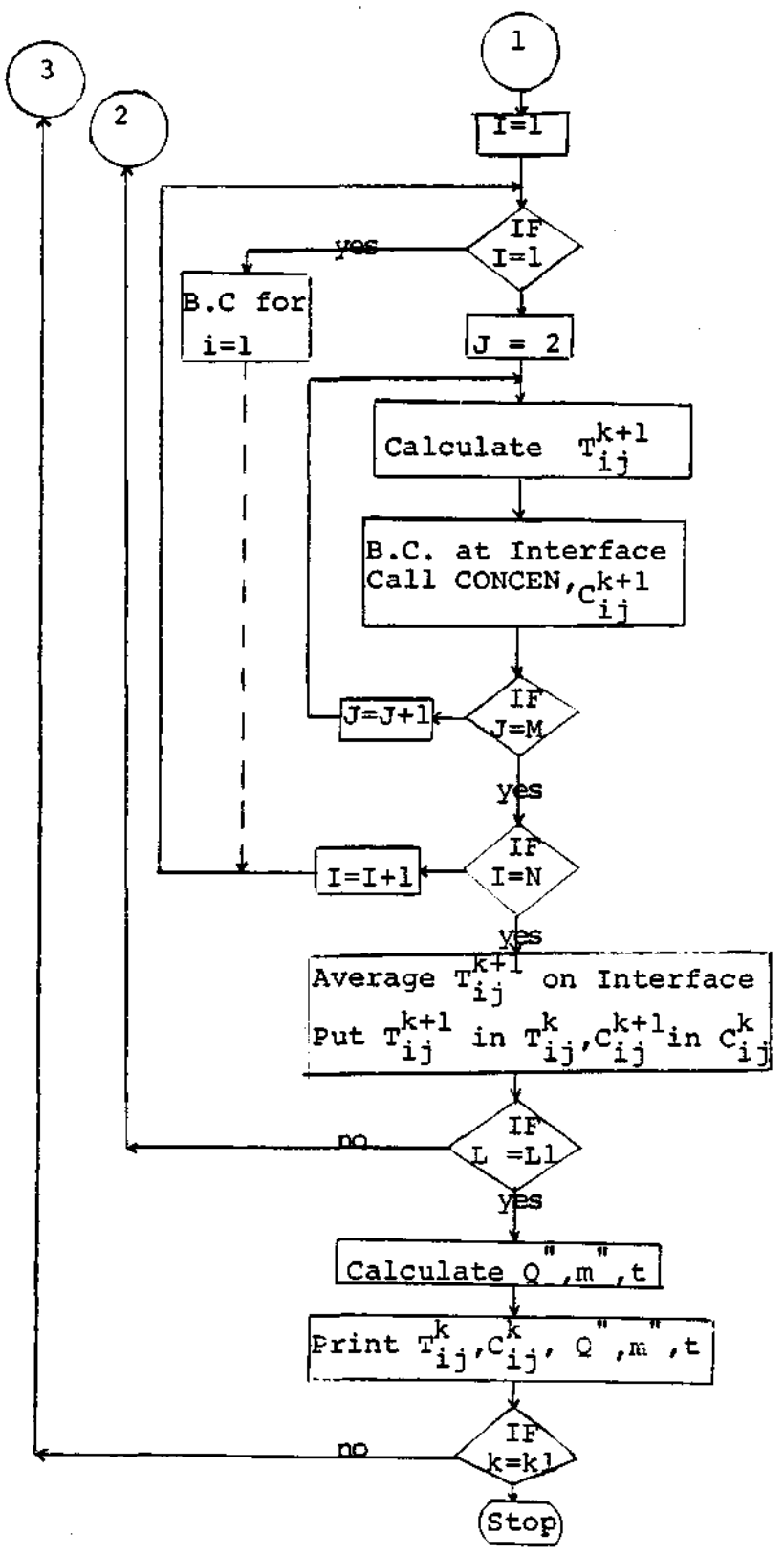
39. Yao,S.C.and V.E. Schrock,"An Experimental Investigation of Transient Heat and Mass Transfer from Falling Drops," Trans. ASME, J. Heat Transfer, 98, 120-126 (1976).

40. Zahm,A.F., Natl. Advisory Comm. Aeronaut. Rept. 253(1927).

APPENDIX A

Flow Diagram For Heat And Mass Transfer Calculations




1
2
3
I=1
IF I=1
yes
B.C for i=1
J = 2
Calculate T_{ij}^{k+1}
B.C. at Interface
Call CONCEN, C_{ij}^{k+1}
IF J=M
J=J+1
yes
IF I=N
I=I+1
yes
Average T_{ij}^{k+1} on Interface
Put T_{ij}^{k+1} in T_{ij}^{k}, C_{ij}^{k+1} in C_{ij}^{k}
IF L =L1
no
yes
Calculate Q", m", t
Print T_{ij}^{k}, C_{ij}^{k}, Q", m", t
IF k=k1
no
Stop

APPENDICES B & C

This section contains a listing of the computer program. The program consists of the main program and the following sobroutines:

CONCEN - Calculation of the density distribution(21);

VP - Calculation of the vapor pressure of water and the latent heat of vaporization(10);

LIQ - Calculation of the water droplet density;

ATMD - Calculation of the atmosphere density;

DIFF - Calculation of the diffusivity distribution;

FRAC - Calculation of the thermal diffusivity.

APPENDIX B

Program For Heat And Mass Transfer Calculations

```
C  THIS PROGRAM IS WRITTEN TO CALCULATE THE TEMPERATURE AND DENSITY
C DISTRIBUTIONS AROUND WATER DROPLET FALLING THROUGH A STEAM ATMOSPHERE
C DEFINITION OF THE RESPECTIVE SUBROUTINES:
C VP= CALCULATES THE VAPOUR PRESSURE OF WATER,
C ATMD= CALCULATES THE ATMOSPHERE DENSITY,
C DIFF= CALCULATES THE DIFFUSIVITY OF STEAM IN AIR,
C FRAC = CALCULATES THE FRACTION OF STEAM AND AIR IN MIXTURE
C LIQ = CALCULATES THE DENSITY OF WATER DROPLET
C   DEFINITION OF VARIABLES:
C  TINF= TEMPERATURE OF THE AIR/STEAM MIXTURE AT INFINITY,
C  PINF= PRESSURE OF THE AIR/STEAM MIXTURE AT INFINITY,
C  TSUR = INITIAL DROPLET TEMPERATURE,
C  DATM = DENSITY OF THE ATMOSPHERE,
C  TOLD,COLD = DIMENSIONLESS OLD TEMPERATURE AND DENSITY DISTRIBUTIONS
C  TNEW,CNEW = DIMENSIONLESS NEW TEMPERATURE AND DENSITY DISTRIBUTIONS
C  PTOTAL = TOTAL PRESSURE,
C  XSTM = FRACTION OF STEAM IN MIXTURE,
C  XAIR = FRACTION OF AIR IN MIXTURE,
C  DCOF = MOLECULAR DIFFUSIVITY; DTETA=ANGULAR INCREMENT,
C  D = DIAMETER OF DROPLET, DTAU = DIMENSIONLESS TIME INCREMENT,
C  VT = TURBULENT DIFFUSIVITY, DR=RADIAL MESH SIZE,
C  QT = LOCAL HEAT FLUX
C  TTK = TOTAL CONDUCTIVITY
C  TQM = LOCAL MASS FLUX
C  DABT = TOTAL DIFFUSIVITY
      DIMENSION TOLD(41,31),TNEW(41,31),R(41),G(41),A(41,31),
     1 E(41,31),F(41,31),UR(42,32),UTETA(42,32),B(41,31),ANGLE(31),
     1AA(41,31),BB(41,31),CC(41,31),DD(41,31),Q(41,31),QT(31),VT(41,31),
     1QTCON1(31),GI(41),HD(31),DABT(41,31),COLD(41,31),CNEW(41,31),
     2PZ(31),TQM(31),QII(31),TTK(31),VTT(41,31),DABT1(31),HSEN(31)
      COMMON UR,UTETA,VT,A,B,GI,G,E,F,DATM,TINF,TATM,TZERO,DSUR,N,
     1 M,DTAU,DTETA,DR,T2,R.
      INTEGER ANGLE
C   READ IN THE INITIAL TEMPERATURES OF THE ATMOSPHERE AND THE WATER
C   DROPLET; DROPLET DIAMETER; AND THE NUMBER OF MESH POINTS IN THE
C   RADIAL AND ANGULAR DIRECTIONS RESPECTIVELY.
      READ(5,100) TATM,TZERO,D,N,M
      NP1=N+1
      MP1=M+1
      MM1=M-1
      NP2=N+2
      MP2=M+2
C   VALUE ASSIGNMENT TO TIME, ANGLE, AND RADIUS INCREMENT THAT OBEY
C   THE STABILITY CRITERION.
      DTAU=0.0026
      DTETA=.1047
      DR=.1
      T=DTAU/(DR**2)
      T1=DTAU/(2.*DR)
      T2=DTAU/(2.*(DTETA**2))
      T3=DTAU/(2.*DTETA)
C   INITIALISE THE TEMPERATURE FIELD USING THE DIMENSIONLESS
C   TEMPERATURE NOTATION: 1 FOR HOT REGION AND 0 FOR COLD DROP SURFACE.
      TIME=0.0
      DO 2 I=1,N
```

```
      DO 2 J=1,MP1
      COLD(I,J)=1.0
    2 TOLD(I,J) = 1.0
      DO 3 JJ=1,MP1
      COLD(NP1,JJ)=0.0
    3 TOLD(NP1,JJ)=0.0
      DO 4 MJ=MP1,1,-1
      ANGLE(MJ)=NINT((MJ-1)*DTETA*180./3.1415927)
    4 CONTINUE
C   READ IN THE VELOCITY COMPONENTS FROM THE DATA FILE.
      DO 5 L=1,MP1
      READ(21,101)(UR(K,L),K=NP1,27,-1)
    5 CONTINUE
      DO 6 IL=1,MP1
      READ(8,101)(UTETA(KI,IL),KI=NP1,27,-1)
    6 CONTINUE
      DO 7 II=26,1,-1
      DO 7 IJ=1,MP1
      UR(II,IJ)=UR(27,IJ)
      UTETA(II,IJ)=UTETA(27,IJ)
    7 CONTINUE
C   CALCULATION OF INITIAL PROPERTIES
      TINF=TATM+273.16
      TSUR=TZERO+273.16
      CALL VP(TINF,PINF,HFG)
      CALL LIQ(TZERO,DLIQ)
      CALL FRAC(TSUR,TINF,PINF,PTOTAL,XSTM,XAIR,ALPHA,DSUR)
      CALL ATMD(TINF,XSTM,XAIR,DATM)
      DO 8 I2=1,NP1
    8 R(I2)=1.+(NP1-I2)*DR
C   CALCULATION OF THE TURBULENT DIFFUSIVITY FIELD
      AA(1,1)=UR(1,1)/R(1)
      BB(1,1)=UTETA(2,1)/DR-UTETA(1,1)/R(1)+UR(1,2)/(R(1)*DTETA)
      CC(1,1)= UR(2,1)/DR
      DD(1,1)=UTETA(1,2)/(R(1)*DTETA)+UR(1,1)/R(1)
      UR(NP2,1)=-UR(N,1)
      UTETA(NP2,1)=-UTETA(N,1)
      UR(1,MP2)=-UR(1,M)
      UTETA(1,MP2)=-UTETA(1,M)
      DO 9 I=2,NP1
      UTETA(I,MP2)=-UTETA(I,M)
      UR(I,MP2)=-UR(I,M)
      AA(I,1)=UR(I,1)/R(I)
      CC(I,1)=(UR(I-1,1)-UR(I+1,1))/(2.*DR)
      BB(I,1)=(UTETA(I-1,1)-UTETA(I+1,1))/(2.*DR)-UTETA(I,1)/R(I)+
     1UR(I,2)/(R(I)*DTETA)
      DD(I,1)=UTETA(I,2)/(R(I)*DTETA)+UR(I,1)/R(I)
      DO 9 K=2,MP1
      UR(NP2,K)=-UR(N,K)
      UTETA(NP2,K)=-UTETA(N,K)
      AA(1,K)=UR(1,K)/R(1)
      CC(1,K)=UR(2,K)/DR
      BB(1,K)=UTETA(2,K)/DR-UTETA(1,K)/R(1)+(UR(1,K-1)-UR(1,K+1))
     1/(2.*R(1)*DTETA)
      DD(1,K)=(UTETA(1,K-1)-UTETA(1,K+1))/(2.*R(1)*DTETA)+UR(1,K)/R(1)
```

```
      AA(I,K)=UR(I,K)/R(I)
      BB(I,K)=(UTETA(I-1,K)-UTETA(I+1,K))/(2.*DR)-UTETA(I,K)/R(I)+(UR(
     11,K-1)-UR(I,K+1))/(2.*R(I)*DTETA)
      CC(I,K)=(UR(I-1,K)-UR(I+1,K))/(2.*DR)
    9 DD(I,K)=(UTETA(I,K-1)-UTETA(I,K+1))/(2.*R(I)*DTETA)+UR(I,K)/R(I)
      DO 10 I=1,NP1
      DO 10 K=1,MP1
      Q(I,K)=2.*((AA(I,K)**2)+(CC(I,K)**2)+(DD(I,K)**2))+(BB(I,K)**2)
      VT(I,K)=0.113*ALPHA*(Q(I,K)**0.5)
   10 CONTINUE
      CALL DIFF(TINF,N,M,VT,XAIR,XSTM,DATM,DABT,TTK)
      WRITE(6,104)
      DO 11 J=MP1,1,-1
   11 WRITE(6,105) ANGLE(J), (VT(I,J),I=NP1,1,-1)
      T4=4.69E2*D*DTAU/(TATM-TZERO)
      T5=(TATM-TZERO)/(D*DR)
      T6=(DATM-DSUR)/(D*DR)
      DO 12 JY=1,MP1
      DABT1(JY)=0.5*(DABT(NP1,JY)+DABT(N,JY))
      HD(JY)=2.*TTK(JY)*T5
    12 PZ(JY)=2.*HFG*T6*DABT1(JY)
      DO 13 I1=1,N
      A(I1,1)=T+T1*(2./R(I1)-UR(I1,1))
      A(I1,MP1)=T+T1*(2./R(I1)-UR(I1,MP1))
      B(I1,1)=T-T1*(2./R(I1)-UR(I1,1))
      B(I1,MP1)=T-T1*(2./R(I1)-UR(I1,MP1))
      DO 13 J1=2,M
      A(I1,J1)=T+T1*(2./R(I1)-UR(I1,J1))
      B(I1,J1)=T-T1*(2./R(I1)-UR(I1,J1))
      GI(I1)=1.-2.*T-T2/(R(I1)**2)
      G(I1)=1.-2.*T-4.*T2/(R(I1)**2)
      E(I1,J1)=2.*T2/(R(I1)**2)-T3*(1./(TAN((J1-1)*DTETA)*(R(I1)**2))-
     1 UTETA(I1,J1)/R(I1))
      F(I1,J1)=2.*T2/(R(I1)**2)+T3*(1./(TAN((J1-1)*DTETA)*(R(I1)**2))-
     2 UTETA(I1,J1)/R(I1))
   13 CONTINUE
C  CARRY OUT FINITE DIFFERENCE CALCULATION OF TIME DEPENDENT
C  TEMPERATURE DISTRIBUTION OUTSIDE THE DROPLET
      TAU=0.0
      DO 14 N1=1,20
      ICOUNT=0
   15 ICOUNT=ICOUNT+1
      TAU = TAU + DTAU
      CALL CONCEN(TOLD,COLD,CNEW)
      DO 16 I=1,N
      IF(I.EQ.1) GOTO 17
      DO 18 J=2,M
      TNEW(I,J)=A(I,J)*TOLD(I+1,J)+B(I,J)*TOLD(I-1,J)+G(I)*TOLD(I,J)
     1 +E(I,J)*TOLD(I,J-1)+F(I,J)*TOLD(I,J+1)
      TNEW(I,1)=A(I,1)*TOLD(I+1,1)+B(I,1)*TOLD(I-1,1)+GI(I)*TOLD(I,1)+
     1 (T2/(R(I)**2))*TOLD(I,3)
      TNEW(I,MP1)=A(I,MP1)*TOLD(I+1,MP1)+B(I,MP1)*TOLD(I-1,MP1)+GI(I)*
     2 TOLD(I,MP1)+(T2/(R(I)**2))*TOLD(I,MM1)
C   BOUNDARY CONDITION AT THE DROP SURFACE
C  FOR CALCULATION WE ASSUME THE LATENT HEAT OF VAPORIZATION
```

```
C  AS CALCULATED IN SUBROUTINE VP.
       TNEW(1,J)=1.0
       QT(J)=HD(J)*(TOLD(N,J)-TOLD(NP1,J))+PZ(J)*(COLD(N,J)-COLD(NP1,J))
       QT(1)=HD(1)*(TOLD(N,1)-TOLD(NP1,1))+PZ(1)*(COLD(N,1)-COLD(NP1,1))
       QT(MP1)=HD(MP1)*(TOLD(N,MP1)-TOLD(NP1,MP1))+PZ(MP1)*(COLD(N,MP1)-
     1 COLD(NP1,MP1))
       TNEW(NP1,J)=TOLD(NP1,J)+T4*QT(J)*(COS((FLOAT(J-1)-0.5)*DTETA)-COS
     1((FLOAT(J-1)+0.5)*DTETA))
       TNEW(NP1,1)=TOLD(NP1,1)+T4*QT(1)*(COS(-0.5*DTETA)-COS(0.5*DTETA))
       TNEW(NP1,MP1)=TOLD(NP1,MP1)-T4*QT(MP1)*(COS(30.5*DTETA)-COS(31.5*
     2DTETA))
       TOM(J)=2.*DABT1(J)*T6*(COLD(N,J)-COLD(NP1,J))
       TOM(1)=2.*DABT1(1)*T6*(COLD(N,1)-COLD(NP1,1))
       TOM(MP1)=2.*DABT1(MP1)*T6*(COLD(N,MP1)-COLD(NP1,MP1))
  18   CONTINUE
  17   TNEW(1,1)=1.0
       TNEW(1,MP1)=1.0
  16   CONTINUE
       SUM=0.0
       SUM1=0.0
       DO 19 J1=1,MP1
       SUM1=SUM1+TNEW(NP1,J1)
       SUM=SUM+CNEW(NP1,J1)
  19   CONTINUE
       CNEWAV=SUM/(FLOAT(MP1))
       TNEWAV=SUM1/(FLOAT(MP1))
C   EQUATE TNEW TO CORRESPONDING TOLD FOR THE NEXT ITERATION.
       DO 20 KK=1,N
       DO 20 NN=1,MP1
       COLD(KK,NN)=CNEW(KK,NN)
  20   TOLD(KK,NN)=TNEW(KK,NN)
       DO 21 JA=1,MP1
       COLD(NP1,JA)=CNEWAV
  21   TOLD(NP1,JA)=TNEWAV
C   START THE ITERATION.
       IF(ICOUNT.NE.10) GOTO 15
       SUM2=0.0
       SUM3=0.0
       DO 22 JI=1,MP1
       QTCON1(JI)=HFG*TOM(JI)
       HSEN(JI)=QT(JI)-QTCON1(JI)
       SUM2=SUM2+HSEN(JI)
  22   SUM3=SUM3+TOM(JI)
       SUM2A=SUM2/(FLOAT(MP1))
       SUM3A=SUM3/(FLOAT(MP1))
       QTCON=HFG*SUM3A
C   WRITE OUT THE DIMENSIONLESS TIME;TEMPERATURE AND DENSITY
C   DISTRIBUTIONS FOR THE CURRENT ITERATION.
       WRITE(6,102)
       WRITE(6,106) TNEWAV,CNEWAV,SUM2A,QTCON,SUM3A
       ALPH=1.60E-3/(1.*DLIQ)
       TIME=TAU*(D**2)/(4.*ALPH)
       WRITE(6,109) TIME
       DO 23 J=MP1,1,-1
  23    WRITE(6,107) ANGLE(J),(TNEW(I,J),I=NP1,1,-4)
```

```
      WRITE(6,102)
      WRITE(6,108)
      DO 24 JI=MP1,1,-1
   24 WRITE(6,107) ANGLE(JI),(CNEW(K,JI),K=NP1,1,-4)
   14 CONTINUE
C  FORMATS FOR INPUT AND OUTPUT STATEMENTS
  100 FORMAT(3E10.2,2I2)
  101 FORMAT(15F5.2)
  102 FORMAT(///)
  104 FORMAT(1H1,26X,'TURBULENT DIFFUSIVITY DISTRIBUTION'//41X,'DIMENSI
     1ONLESS RADIUS'//2X,'ANGLE     1.0     1.1     1.2     1.3     1.4
     1     1.5     1.6     1.7     1.8     1.9     2.0'/)
  105 FORMAT(I6,2X,11F8.4/8X,11F8.4/8X,11F8.4/8X,8F8.4)
  106 FORMAT(10X,'AVERAGE VALUES OF DROPLET TEMPERATURE,DENSITY;TOTAL H
     1EAT FLUX,CONDENSIVE HEAT FLUX AND MASS FLUX'//36X,'SURFACE TEMPERA
     2TURE =',F8.4/36X,'SURFACE DENSITY =',F8.4/36X,'SENSI-HEAT FLUX =',
     3E10.2,'CAL/SEC-SQCM'/36X,'CONDENSIVE HEAT FLUX =',E10.2,'CAL/SEC-S
     4QCM'/36X,'MASS FLUX =',E10.2,'GM/SEC-SQCM'/)
  107 FORMAT(I6,2X,11F8.4)
  108 FORMAT(1H1,26X,'DENSITY DISTRIBUTION AROUND THE DROPLET'//41X,'DI
     1MENSIONLESS RADIUS'//2X,'ANGLE     1.0     1.4     1.8     2.2
     2 2.6     3.0     3.4     3.8     4.2     4.6     5.0'/)
  109 FORMAT(1H1,2X,'WHEN TIME =',F11.9,'SEC'//26X,'TEMPERATURE DISTRIBU
     1TION AROUND THE DROPLET'///41X,'DIMENSIONLESS RADIUS'//2X,'ANGLE
     1    1.0     1.4     1.8     2.2     2.6     3.0     3.4     3.8
     1 4.2     4.6     5.0'/)
      STOP
      END
```

APPENDIX C

Program For Turbulent Diffusivity & Density Calculations

```
      SUBROUTINE CONCEN(TOLD,COLD,CNEW)
      DIMENSION COLD(41,31),CNEW(41,31),R(41),G(41),A(41,31),E(41,31),
     1 F(41,31),UR(42,32),UTETA(42,32),B(41,31),GI(41),VT(41,31),SH(31),
     2 DABT(41,31),PDROP(31),TDROP(31),RG(31),TOLD(41,31)
      COMMON UR,UTETA,VT,A,B,GI,G,E,F,DATM,TINF,TATM,TZERO,DSUR,N,
     1 M,DTAU,DTETA,DR,T2,R
      MP1=M+1
      NP1=N+1
      MM1=M-1
      DO 2 I=1,N
      IF (I.EQ.1) GOTO 3
      DO 4 J=2,M
      CNEW(I,J)=A(I,J)*COLD(I+1,J)+B(I,J)*COLD(I-1,J)+G(I)*COLD(I,J)+
     1 E(I,J)*COLD(I,J-1)+F(I,J)*COLD(I,J+1)
      CNEW(I,1)=A(I,1)*COLD(I+1,1)+B(I,1)*COLD(I-1,1)+GI(I)*COLD(I,1)+
     2 (T2/(R(I)**2))*COLD(I,3)
      CNEW(I,MP1)=A(I,MP1)*COLD(I+1,MP1)+B(I,MP1)*COLD(I-1,MP1)+GI(I)*
     1 COLD(I,MP1)+(T2/(R(I)**2))*COLD(I,MM1)
      CNEW(1,J)=1.0
C  BOUNDARY CONDITION AT DROPLET SURFACE
      TDROP(J)=TINF-(1.-TOLD(NP1,J))*(TATM-TZERO)
      TDROP(1)=TINF-(1.-TOLD(NP1,1))*(TATM-TZERO)
      TDROP(MP1)=TINF-(1.-TOLD(NP1,MP1))*(TATM-TZERO)
      RG(J)=485.27-0.07966*TDROP(J)
      RG(1)=485.27-0.07966*TDROP(1)
      RG(MP1)=485.27-0.07966*TDROP(MP1)
      PDROP(J)=6.0573E26*(TDROP(J)**(-5.3512))*EXP(-6890.81/TDROP(J))
      PDROP(1)=6.0573E26*(TDROP(1)**(-5.3512))*EXP(-6890.81/TDROP(1))
      PDROP(MP1)=6.0573E26*(TDROP(MP1)**(-5.3512))*EXP(-6890.81/TDROP(
     1MP1))
      CNEW(NP1,J)=1.E-3*PDROP(J)/(TDROP(J)*RG(J)*(DATM-DSUR))-DSUR/(
     1DATM-DSUR)
      CNEW(NP1,1)=1.E-3*PDROP(1)/(TDROP(1)*RG(1)*(DATM-DSUR))-DSUR/(
     2DATM-DSUR)
      CNEW(NP1,MP1)=1.E-3*PDROP(MP1)/(TDROP(MP1)*RG(MP1)*(DATM-DSUR))-
     3DSUR/(DATM-DSUR)
4     CONTINUE
3     CNEW(1,1)=1.0
      CNEW(1,MP1)=1.0
2     CONTINUE
      RETURN
      END
      SUBROUTINE VP(T,P,HFG)
      P=((T/373.15)**13.8)+2.5E-4*(T-373.15)
      HFG=538.97+0.594*(373.15-T)
      RETURN
      END
      SUBROUTINE LIQ(T,DLIQ)
      VLIQ=1.0018+0.0002615*(T-20.)+(3.219E-6)*((T-20.)**2)
      DLIQ=1./VLIQ
      RETURN
      END
      SUBROUTINE ATMD(T,XSTM,XAIR,DATM)
      DAIR=0.001185
      RG=485.27-0.07966*T
```

```
      P=6.0573E26*(T**(-5.3512))*EXP(-6890.81/T)
      DSTM=1.E-3*P/(T*RG)
      B1=XSTM*DSTM*SQRT(18.)+XAIR*DAIR*SQRT(29.)
      B2=XSTM*SQRT(18.)+XAIR*SQRT(29.)
      DATM=B1/B2
      RETURN
      END
      SUBROUTINE FRAC(T,T1,P,PTOTAL,XSTM,XAIR,ALPHA,D)
      PAIR=T1/298.16
      PTOTAL=P+PAIR
      XAIR=PAIR/PTOTAL
      XSTM = 1.0-XAIR
      A=T**2
      B=T**3
      CP=1.943-8.92E-3*T+1.7867E-5*A-1.183E-8*B
      TK=2.445E-5-1.96E-8*T+3.367E-10*A-1.077E-13*B
      RG=485.27-0.07966*T
      P1=6.0573E26*(T**(-5.3512))*EXP(-6890.81/T)
      D=1.E-3*P1/(T*RG)
      ALPHA=TK/(D*CP)
      RETURN
      END
      SUBROUTINE DIFF(T,N,M,VT,XAIR,XSTM,DATM,DABT,TTK)
      DIMENSION VT(41,31),DABT(41,31),TTK(31)
      MP1=M+1
      NP1=N+1
      DCOF=5.385E-6*(T**1.88)
      CP=1.943-8.92E-3*T+1.7867E-5*(T**2)-1.183E-8*(T**3)
        TK=((7.56E-4)*XAIR*(29.**.333)+(6.57E-4)*XSTM*(18.**.333))/(XSTM
     1*(18.**.333)+XAIR*(29.**.333))
        TZ=CP*DATM
        DO 4 K=1,NP1
        DO 4 L=1,MP1
    4   DABT(K,L)=DCOF*VT(K,L)
        DO 5 J=1,MP1
    5   TTK(J)=TK+0.5*TZ*(VT(NP1,J)+VT(N,J))
        RETURN
        END
```

APPENDIX D

CALCULATION TECHNIQUE OF THE VELOCITY COMPONENTS

A streamline is tangent to the velocity of the fluid particles at every point. In steady flow the velocity U with components U_r and U_θ at a given point is constant in time. In Fig. D(i), we have drawn a tube of flow around the droplet. The velocity of the fluid will in general have different magnitudes at different points along the tube. Since in steady flow no fluid can leave through the walls nor can fluid particles temporarily accumulate, the mass crossing each section of the tube per unit time must be the same.

$$AU = \text{constant} \qquad (1)$$

noting that the fluid is incompressible.

We used as our reference velocity that of the far end, U_∞; which when made dimensionless becomes unity. Thus, Eq.1 in dimensionless form becomes

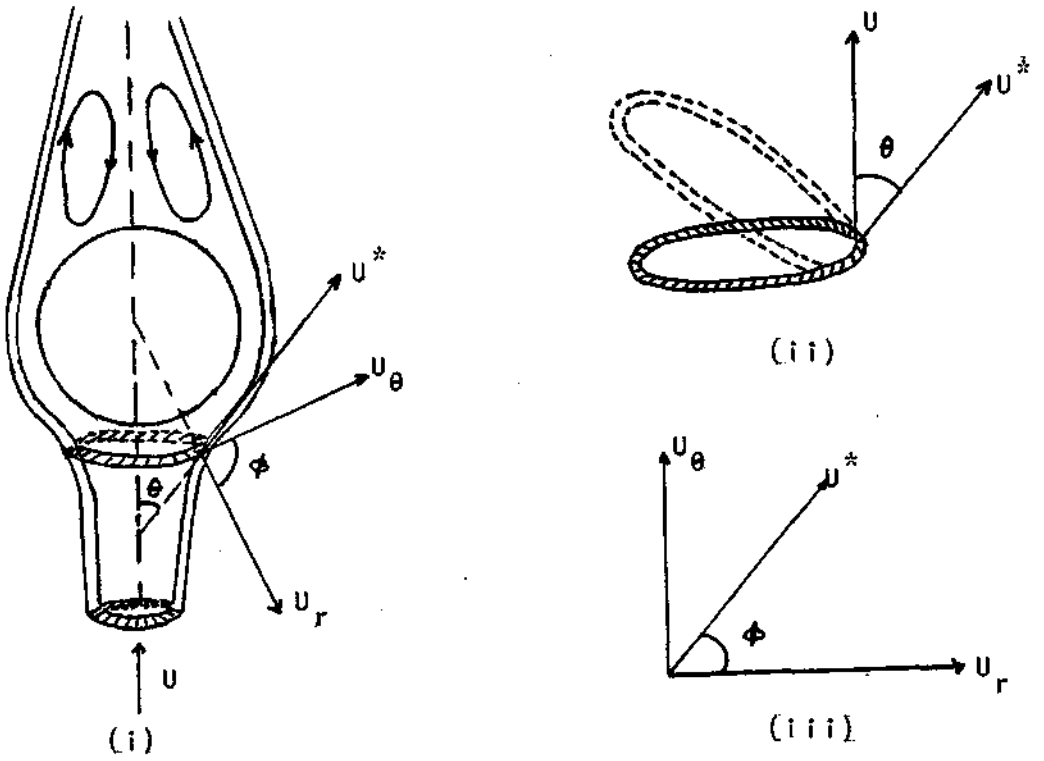


FIGURE D:A Tube of Flow used in computation of Velocity Components

$$U = A_\infty / A \qquad (2)$$

where A_∞ and A are the cross-sectional areas of the tube perpendicular to the streamlines at the far end and any other section respectively, and assuming that the speed is essentially constant over each surface separately. In Fig.D(ii), θ is the angle between the initial velocity U and the final velocity U^*. From Fig.D(ii) and Eq.2, we have

$$\begin{aligned} U^* &= U/\cos\theta \\ &= A_\infty/A\cos\theta \end{aligned} \qquad (3)$$

In Fig.D(iii), this new velocity is now resolved into the two components U_r and U_θ; ϕ is the angle between U^* and U_r :

$$\begin{aligned} U_r &= U^*\cos\phi \\ &= A_\infty\cos\phi/A\cos\theta \end{aligned} \qquad (4)$$

and

$$U_\theta = A_\infty\sin\phi/A\cos\theta \qquad (5)$$

The angles were measured manually. As a numerical example, from Fig.3.1, at polar angle of 60°, and at dimensionless radial position of 1.4, we have $A_\infty/A = 0.96$, $\theta = 15^\circ$, $\phi = 110^\circ$. Substituting these values into Eq.4 and Eq.5 gives

$$U_r = -0.339$$

$$U_\theta = 0.934$$

which agree with the values presented in Tables 5.6 and 5.7 respectively.